Meiosis-specific functions of kinetochore protein SPC105R required for chromosome segregation in *Drosophila* oocytes

Jay N. Joshi, Neha Changela, Lia Mahal, Janet Jang, Tyler Defosse, Lin-Ing Wang, Arunika Das, Joanatta G. Shapiro, and Kim McKim*
Waksman Institute and Department of Genetics, Rutgers, the State University of New Jersey, Piscataway, NJ 08854

ABSTRACT The reductional division of meiosis I requires the separation of chromosome pairs towards opposite poles. We have previously implicated the outer kinetochore protein SPC105R/KNL1 in driving meiosis I chromosome segregation through lateral attachments to microtubules and coorientation of sister centromeres. To identify the domains of SPC105R that are critical for meiotic chromosome segregation, an RNAi-resistant gene expression system was developed. We found that the SPC105R C-terminal domain (aa 1284-1960) is necessary and sufficient for recruiting NDC80 to the kinetochore and building the outer kinetochore. Furthermore, the C-terminal domain recruits BUBR1, which in turn recruits the cohesion protection proteins MEI-S332 and PP2A. Of the remaining 1283 amino acids, we found the first 473 are most important for meiosis. The first 123 amino acids of the N-terminal half of SPC105R contain the conserved SLRK and RISF motifs that are targets of PP1 and Aurora B kinase and are most important for regulating the stability of microtubule attachments and maintaining metaphase I arrest. The region between amino acids 124 and 473 are required for lateral microtubule attachments and biorientation of homologues, which are critical for accurate chromosome segregation in meiosis I.

SIGNIFICANCE STATEMENT

- Kinetochore proteins regulate meiosis specific functions. SPC105R is a central regulator of kinetochore function but its role in meiosis is not well understood.

- We identified regions of SPC105R that regulate key meiosis I functions, including sister centromere fusion and kinetochore-microtubule interactions.

- SPC105R is a hub that recruits several proteins to regulate kinetochore activity. Future work will involve identifying the proteins recruited by SPC105R that mediate these functions in meiosis.

INTRODUCTION

Kinetochores are large protein complexes built on top of the centromeres that interact with microtubules and regulate cell-cycle progression (Musacchio and Desai, 2017; McAinsh and Marston, 2022). The conserved KMN (Knl1-Mis12-Ndc80) network is required for kinetochore–microtubule attachments (KT–MT) in vivo and is composed of three groups of proteins: Spc105/KNL1, the Mis12 complex, and the Ndc80 complex (NDC80c; Przewloka and Glover, 2009). SPC105R is the *Drosophila* homologues of KNL1

(Schittenhelm et al., 2009) and is required for outer kinetochore assembly in oocytes (Radford et al., 2015). Within the KMN network, two microtubule binding sites have been identified, in Ndc80 and Spc105/KNL1 (Cheeseman et al., 2006). In addition to facilitating microtubule attachments, KNL1 serves as a scaffold to recruit spindle assembly checkpoint proteins (Caldas and DeLuca, 2014). Spc105R/KNL1 thus has a critical role in regulating cell division.

Meiosis I results in a reduction of ploidy as homologous chromosomes segregate into daughter cells, which is distinct from the segregation of sister chromatid in meiosis II and mitosis. Thus, homologous chromosome segregation in meiosis I involves unique chromosome-based mechanisms (Paliulis and Nicklas, 2000). SPC105R regulates two meiosis I functions: coorientation of sister chromatids and biorientation of homologous chromosomes (Radford et al., 2015). Coorientation requires the fusion of fusing sister kinetochores during prometaphase I. Regulation of cohesion loss is a critical component that differentiates the two meiotic divisions. Arm cohesion is lost in meiosis I, but centromeric cohesion must be maintained until meiosis II (Ogushi et al., 2021). Failure to fuse sister kinetochores results in merotelic attachments, with one pair of sister chromatids attached to both spindle poles (Watanabe, 2012; Nasmyth, 2015). We previously found that coorientation depends on two independent mechanisms, regulation of end-on microtubule attachments and centromeric cohesion (Wang et al., 2019). How SPC105R regulates meiotic cohesion, and microtubule attachments, is not known.

Biorientation is a critical part of prometaphase I that establishes how pairs of homologous chromosome segregate at anaphase I. Pairs of homologous chromosomes, joined by chiasmata, biorient on a bipolar meiotic spindle through attachment of kinetochores to microtubules from opposite poles (Hughes et al., 2018). There are, however, important biological differences between oocytes and other cell types, such as the absence of centrosomes (Dumont and Desai, 2012; Radford et al., 2017; Kitajima, 2018; Mihajlovic and FitzHarris, 2018). Understanding these differences and how they impact the mechanism of biorientation in oocytes might help explain the high error rate in human oocytes (Webster and Schuh, 2017).

Based on differences between oocytes depleted of SPC105R or NDC80, we proposed that acentrosomal spindle have two types of kinetochore-microtubule attachments (Radford et al., 2015). Lateral attachments, where the kinetochores interact with the sides of microtubules, depend on SPC105R. More stable end-on attachments, where kinetochores interact with the ends of microtubules, depend on NDC80. The dependence of oocytes on lateral attachments for biorientation is likely conserved (Wignall and Villeneuve, 2009; Dumont et al., 2010) and present in other cell types (Magidson et al., 2015; Itoh et al., 2018). During prometaphase in mouse oocytes, the chromosomes congress to the central spindle, which promotes biorientation by bringing kinetochores into the vicinity of a high density of microtubule plus ends (Kitajima et al., 2011; Magidson et al., 2011). Similarly, Drosophila oocytes have a robust central spindle that depends on the kinesin-6 Subito, is composed of several proteins including the Aurora B kinase (Jang et al., 2005; Costa and Ohkura, 2019), and is required for error correction and biorientation during prometaphase (Jang et al., 2007; Das et al., 2018). Regulating the transition from lateral to end-on attachment appears to be critical for avoiding biorientation defects in mammals (Yoshida et al., 2015) and Drosophila (Głuszek et al., 2015).

We initiated this study of SPC105R in oocytes to understand how the meiosis-specific functions of kinetochore coorientation and biorientation are regulated. To do this, we generated an RNAi-resistant functional Spc105R transgene and used it as a platform to study mutants with deletions of specific domains. Our results show that the C-terminal domain is sufficient for recruiting outer kinetochore proteins and establishing end-on attachments. It also recruits cohesion protection proteins, which are required to fuse the sister kinetochores during meiosis I. The rest of SPC105R (aa 1-1283) regulates end-on attachments and biorientation. We identified one region in particular, between 123 and 473, that is required for biorientation of homologous chromosomes. Our evidence suggests this region is required for lateral microtubule interactions and regulating the transition from lateral to end-on attachments.

RESULTS

Using RNAi-resistant transgenes to study SPC105R function

There are two Spc105R isoforms predicted from the genome sequence: Spc105R^A and Spc105R^B (Supplemental Figure S1A). Alternative splicing results in different translation start sites, such that the sequence MNANKRRSSLRK in the B form is replaced with MVDLLFLQLRK in the A form. The only known full length cDNA encodes the A form, but multiple 5′ cDNA sequences from RACE experiments correspond to the B form (Gramates et al., 2022). Furthermore, RT-PCR amplification specific to mRNA for each isoform from wild-type female ovaries confirmed the presence of both A and B isoforms (Supplemental Figure S1B). Both isoforms could be detected at the kinetochores when expressed using MYC-tagged transgenes (Supplemental Figure S1C). These results suggest that both isoforms are incorporated into the kinetochore.

To study the function of Spc105R in meiosis, we constructed RNAi-resistant transgenes that contained silent mutations to the bases targeted by the shRNA GL00392 (Figure 1A). While Drosophila females expressing GL00392 in the ovary using matα have reduced Spc105R expression and are sterile, females expressing the RNAi-resistant B-form of SPC105R, Spc105R^B, and GL00392 (to be referred to as Spc105R^B Spc105R^RNAi oocytes) were fertile (Table 1; Supplemental Figure S2). Spc105R^B Spc105R^RNAi females were more fertile than Spc105R^A Spc105R^RNAi females, suggesting that SPC105R^B is the more important isoform for providing functional rescue of Spc105R. Spc105R^B rescued the lethality caused by ubiquitous expression of GL00392 using P{w[+mC] = tubP-GAL4}LL7 (referred to as Tub:GAL4; Figure 1B). This lethality was also suppressed by expression of Spc105R^A, consistent with the conclusion that both isoforms are functional in mitosis.

Oocytes lacking SPC105R are characterized by the loss of several kinetochore proteins and microtubule attachments (Radford et al., 2015; Wang et al., 2019). The absence of KT–MT attachments results in a "hollow spindle" phenotype in which the centromeres lack an association with the microtubules (Figure 1C; Supplemental Figure S2A). All the microtubules are interpolar, with the plus-ends of microtubules from opposite poles making antiparallel overlaps in the center of the spindle. Spc105R^B rescued the attachment defects present in Spc105R^RNAi oocytes (Figure 1C; Supplemental Figure S2A). All the centromeres were observed to make contacts with microtubules, with the majority making end-on attachments to the plus ends of kinetochore microtubules. Spc105R^B also rescued SPC105R localization to the kinetochore, which was significantly reduced in Spc105R^RNAi oocytes (Figure 1C; Supplemental Figure S2, A and B). These results show that Spc105R^B can provide the meiotic and mitotic functions of SPC105R, although due to the absence of the Spc105R^A isoform or differences in expression level, the phenotype is not always identical to wild-type.

Based on sequence comparisons and studies in mitotic embryo cells (Schittenhelm et al., 2009), we divided SPC105R into five regions (Figure 1A). The N-terminal domain includes potential
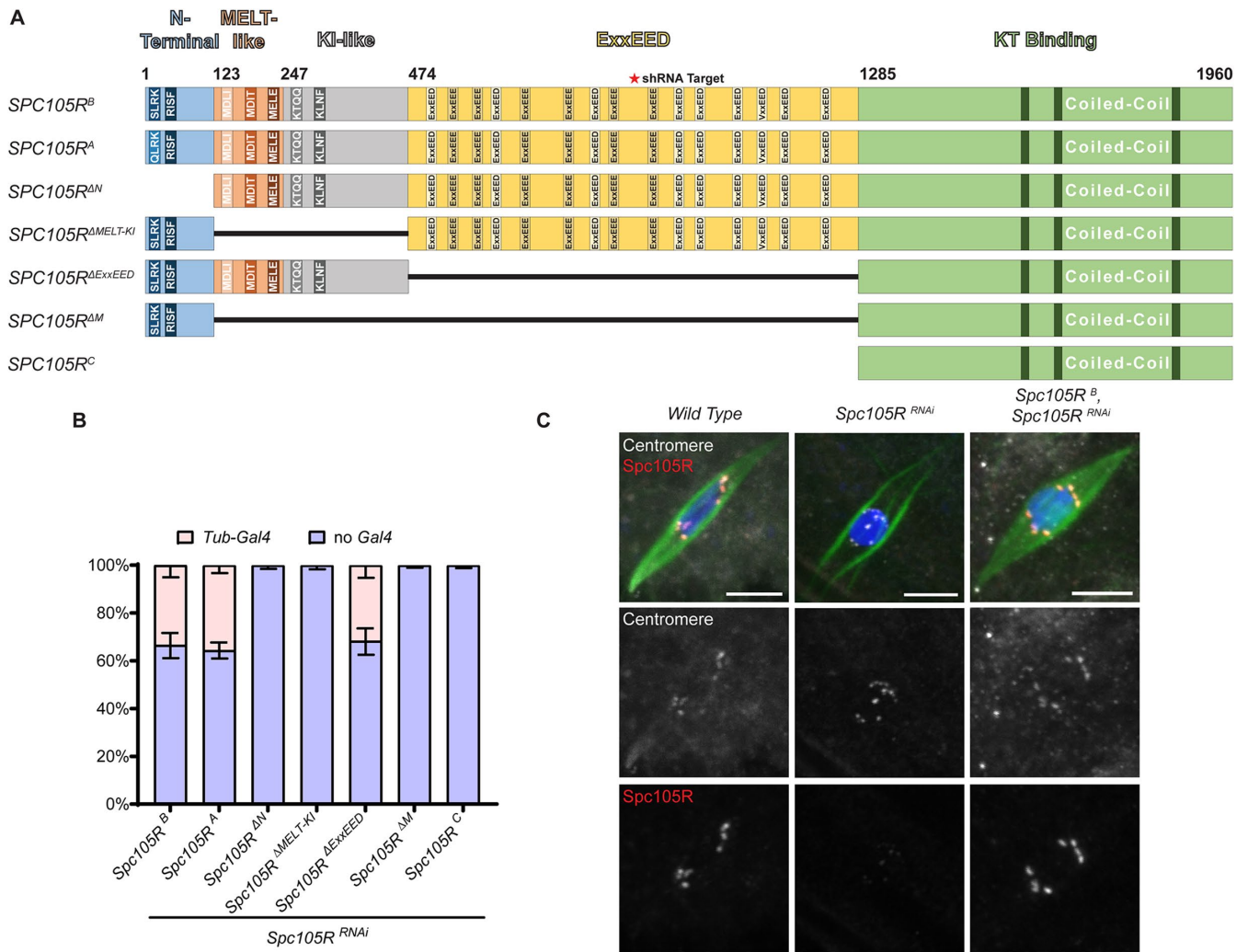
FIGURE 1: *Spc105R^B* rescues the viability and microtubule attachment defects in *Spc105R^RNAi* oocytes. (A) A schematic of the two known *Drosophila Spc105R* isoforms and mutants used in this study. The first nine amino acids in SPC105R^B are changed from MNANKRRSS to MVDLLFLQ in SPC105R ^A. The coordinates on the schematic represent the first amino acid of each domain. The N-terminal includes the SLRK and RISF motifs and is where the two isoforms differ. Following this is a domain with three MELT-like motifs, a region that contains two KI-like repeats, a central domain containing repeats with the consensus ExxEED, and the C-terminal region containing coiled-coil motifs. An ExxEED-like consensus is found in several *Drosophila* species (Tromer *et al.*, 2015) although many organisms, including mammals, have repeats of the MELT motif in this domain. The *Drosophila* ExxEED repeats have been proposed to be phosphomimetic derivatives of the MELT motif (Audett *et al.*, 2022), in part because there is a threonine 5 amino acids upstream of the ExxEED consensus in 14/15 of the repeats, and the 15th is a serine. This threonine is a Aurora B phosphorylation site and is part of the consensus KxRxTLL that is related to the TΩ motif upstream of the MELT motif in other organisms (Tromer *et al.*, 2015). All transgenes included missense mutations to make them resistant to the shRNA GL00392. (B) Viability of *Spc105R* mutants, all in a *Spc105R^RNAi* background. Data shows the relative amounts of progeny expressing the *Spc105R^RNAi* and mutants (*Tub-Gal4)* to siblings that did not (no *Gal4*; *n* > 200). (C) Confocal images of w*ild-type*, *Spc105R^RNAi*, and *Spc105R ^B Spc105R^RNAi* oocytes. Merged images show DNA (blue), Tubulin (green), centromeres (white), and SPC105R (red). Centromeres and SPC105R are shown in separate channels. Scale bars are 5 μm.

Aurora B phosphorylation, PP1, and microtubule binding sites (Audett *et al.*, 2022). Next to the N-terminal domain is a region containing three motifs that are related to the MELT consensus (MDLI, MDIT, and MELE). This is followed by a disordered region that contains two sequences similar to the KI motifs of vertebrate orthologues (Audett *et al.*, 2022; McGory *et al.*, 2024). The central region of the protein contains 15 repeats with the consensus ExxEED. The C-terminal domain was previously shown to be sufficient for recruiting the NDC80c in mitotic cells (Schittenhelm *et al.*, 2009).

Five deletion mutations, one for each domain, were made on the *Spc105R^B* sequence. Each mutant protein was detected by Western blot or cytologically at the centromeres using anti-myc antibodies (Supplemental Figure S1, C–E). However, three mutants were detected by anti-myc but not the anti-SPC10R antibody. The SPC105R antibody was raised against the first 400 amino acids of SPC105R (Schittenhelm *et al.*, 2009). Thus, it is expected that SPC105R^C- would not be detected because that region was deleted. However, the absence of staining in *Spc105R^ΔM*

	Genotype	NDJ (%)	Total
Spc105R^RNAi and	*Spc105R^B*	0.1	2347
	Spc105R^A	0.0	59
	Spc105R^ΔN	–	sterile
	Spc105R^ΔExxEED	10.3 ****	604
	Spc105R^ΔM	–	sterile
	Spc105R^ΔMELT-KI	–	sterile
	Spc105R^C	–	sterile
No RNAi	*Spc105R^B*	0.5	2688
	Spc105R^A	0.3	1051
	Spc105R^ΔN	–	sterile
	Spc105R^ΔExxEED	1.5	528
	Spc105R^ΔM	–	Sterile
	Spc105R^ΔMELT-KI	5.6 ****	460
	Spc105R^C	–	sterile

Females expressing the indicated transgene were either in a *Spc105R^RNAi* or wild-type (dominant) background. Significant levels of bi-orientation defects ($p < 0.001$, Fishers exact test) are shown by ****. NDJ = nondisjunction.

TABLE 1: Fertility and nondisjunction in *Spc105R* domain mutant females.

Spc105R^RNAi and *Spc105R^ΔMELT-KI* *Spc105R^RNAi* oocytes indicates the SPC105R antibody detects a region between amino acids 124 and 473, while the region between 1 and 123 is not detected (Supplemental Figure S2).

The role of SPC105R in homologous chromosome biorientation

To determine the effect of each *Spc105R* mutant on chromosome segregation, we examined homologous chromosome biorientation. Pairs of homologous chromosomes are bi-oriented in metaphase I when their centromeres are oriented towards opposite poles. To measure biorientation, we labeled three of the four *D. melanogaster* chromosomes, the X, 2nd, and 3rd, with fluorescent probes specific for each centromere. A biorientation defect was defined as both FISH signals oriented towards the same pole.

Chromosome biorientation in *Spc105R^B* *Spc105R^RNAi* oocytes was similar to that of wild-type controls (Figure 2). *Spc105R^C* *Spc105R^RNAi* oocytes had a high frequency of biorientation defects (61.9%), suggesting domains or sequences between amino acids 1 and 1284 regulate biorientation or error correction (Figure 2). A deletion of the large region containing ExxEED/E repeats, *Spc105R^ΔExxEED* *Spc105R^RNAi* oocytes, did not have a significant frequency of biorientation defects. Deletion of this region was also fertile, and nondisjunction was observed among the progeny (Table 1). This difference may be due to the sensitivity of the genetic assay, or errors in meiosis II. In contrast, *Spc105R^ΔM* *Spc105R^RNAi*, and *Spc105R^ΔMELT-KI* *Spc105R^RNAi* oocytes had a high frequency of biorientation defects (45.5%) that was similar to *Spc105R^C*. In addition, *Spc105R^ΔMELT-KI* females, where the wild-type protein was present, were fertile and had significant levels of nondisjunction (Table 1). A lower but significant biorientation defect was observed in *Spc105R^ΔN* *Spc105R^RNAi* oocytes (12.8%, $p = 0.0023$; Figure 2). These results suggest that biorientation is primarily mediated by the region between amino acids 124 and 473, while the N-terminal domain has a minor contribution.

The C-terminal domain of SPC105R is sufficient for outer kinetochore assembly

The C-terminal domain of SPC105R, beginning after the last ExxEED/E repeat, was previously defined in mitotic cells as being capable of organizing the kinetochore (Schittenhelm *et al.*, 2009). This KT-binding domain of SPC105R contains coiled-coil motifs which are suspected to drive its localization to the kinetochore and facilitate recruitment of other kinetochore proteins (Liu *et al.*, 2016). In *Spc105R^C*, *Spc105R^RNAi* oocytes, we observed kinetochore localization of SPC105R^C using an antibody to the MYC epitope (Supplemental Figure S1C), showing this domain is sufficient for SPC105R recruitment in oocytes. In addition, when SPC105R^C (and also SPC105R^ΔN or SPC105R^ΔM) was expressed without *Spc105R^RNAi*, both wild-type and mutant proteins were detected at the kinetochore (Supplemental Figure S2C). Incorporation of both wild-type and mutant proteins may explain why these mutants caused dominant sterility, although the effects of overexpression cannot be ruled out (Table 1).

In *Spc105R^RNAi* oocytes, NDC80 does not localize to the kinetochore (Radford *et al.*, 2015; Figure 3A). In contrast, NDC80 localized to the kinetochores in *Spc105R^C* *Spc105R^RNAi* oocytes, indicating that the C-terminal domain of SPC105R is sufficient to build a meiotic kinetochore (Figure 3, A and B). Although *Spc105R^C* *Spc105R^RNAi* oocytes could recruit NDC80 and assemble a kinetochore, the organization of the chromosomes and spindle was abnormal. In wild-type oocytes, all chromosomes coalesce together in a single round or oval karyosome. In *Spc105R^C* *Spc105R^RNAi* oocytes, the karyosomes were often elongated and fragmented (Figure 3, A and C), and contained a mix of end-on (Figure 4, A and C; Supplemental Figure S1) and lateral (Figures 3, A and C; 4E) KT–MT attachments. The karyosome phenotype could be the result of creating a kinetochore that lacks key regulatory components recruited by the rest of SPC105R, resulting in unregulated microtubule attachments and causing the karyosome to elongate or fragment.

To determine whether the karyosome elongation phenotype was caused by the unregulated formation of end-on KT–MT attachments, we examined *Spc105R^C* *Spc105R^RNAi* oocytes also depleted for NDC80. The rationale for this experiment was that end-on attachments do not form in *Ndc80^RNAi* oocytes (Radford *et al.*, 2015). In *Spc105R^C* *Spc105R^RNAi* *Ndc80^RNAi* oocytes, the karyosomes were spherical and shorter in length compared with *Spc105R^C* *Spc105R^RNAi* oocytes (Figure 3, C and D). Because NDC80 depletion suppressed the *Spc105R^C* *Spc105R^RNAi* phenotype, it is likely that unregulated NDC80-dependent end-on attachments were responsible for the karyosome elongation and separation observed in *Spc105R^C* *Spc105R^RNAi* oocytes.

The C-terminal domain of SPC105R recruits proteins for maintaining cohesion

Coorientation is the process to ensure sister kinetochores fuse and orient to the same pole in meiosis I (Watanabe, 2012). A coorientation defect can result in merotelic attachments and errors in homologous chromosomes segregation. We previously showed that two mechanisms maintain coorientation: sister centromere cohesion and the stability of end-on KT–MT attachments (Wang *et al.*, 2019). SPC105R prevents premature centromeric cohesion loss by recruiting MEI-S332, which is the *Drosophila* orthologue of Shugoshin (SGO; Figure 4, A and B; Wang *et al.*, 2019).

Deletion mutants of *Spc105R* were used to investigate which domain recruit cohesion protection proteins. In *Spc105R^C* *Spc105R^RNAi* oocytes, MEI-S332 was localized to the kinetochore. These results show that the C-terminal domain of SPC105R recruits MEI-S332 to
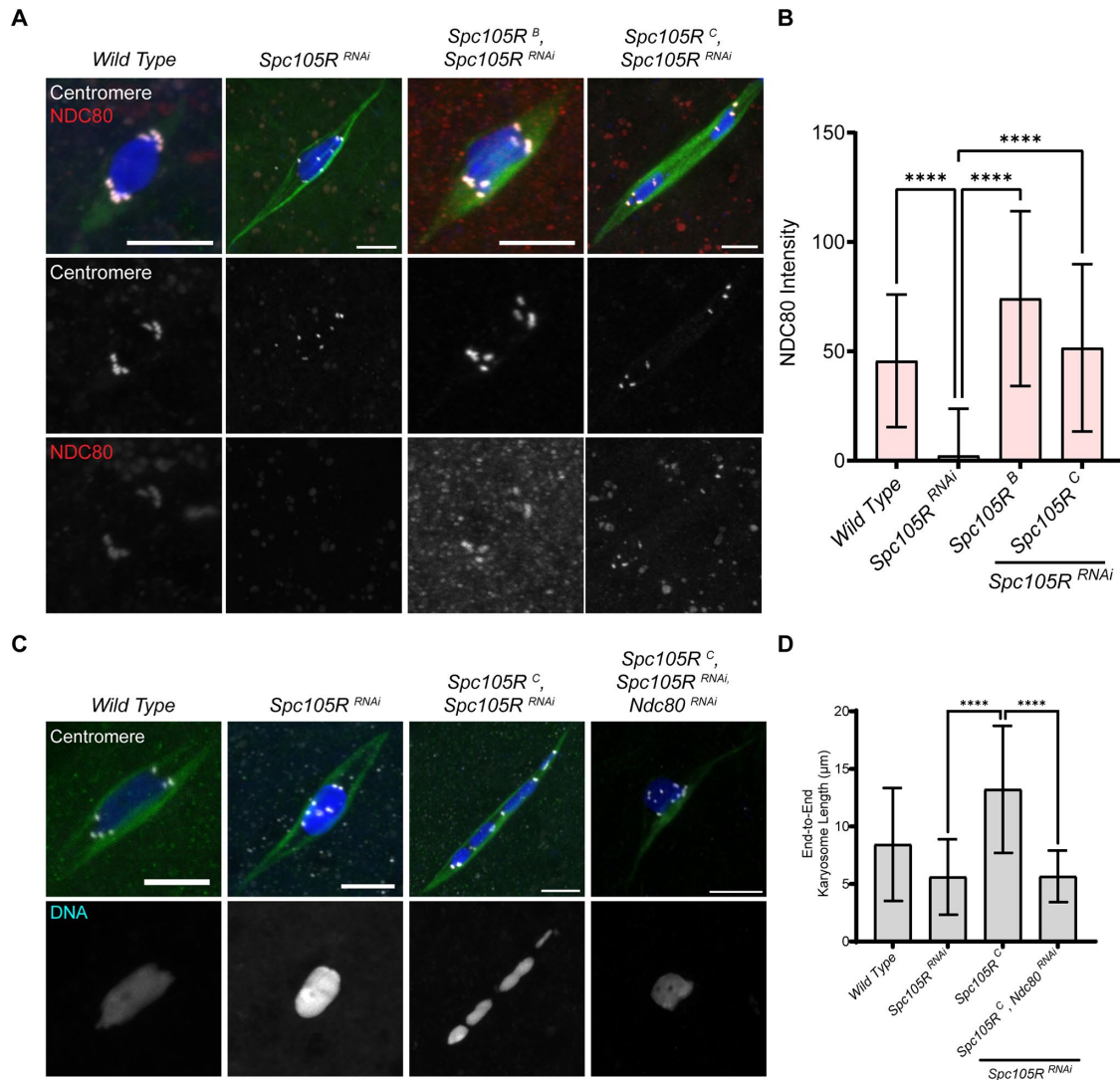
FIGURE 2: Homologous chromosome bi-orientation in *Spc105R* mutants lacking specific domains. (A) Confocal images of *Spc105R^RNAi* oocytes expressing the indicated transgene. Merged images show DNA (blue), Tubulin (green), the X-Chromosome (yellow), the second chromosome (red), and the third chromosome (white). DNA and FISH probes are shown in a separate channel. Scale bars are 5 μm. Examples of monooriented centromeres are circled. (B) Quantification for percent of chromosome monoorientation: *Spc105R ^B Spc105R^RNAi* oocytes ($n = 93$), *Spc105R ^ΔN Spc105R^RNAi* oocytes ($n = 117$), *Spc105R ^ΔMELT-KI Spc105R^RNAi* oocytes ($n = 123$), *Spc105R ^ΔExxEED Spc105R^RNAi* oocytes ($n = 65$), *Spc105R ^ΔM Spc105R^RNAi* oocytes ($n = 81$), *Spc105R ^C Spc105R^RNAi* oocytes ($n = 63$). Significance in frequency of monoorientation in oocytes determined by Fisher's exact test, with * = p values < 0.01, **** = p value < 0.0001.

the kinetochore. SGO maintains cohesion by recruiting PP2A-B56, which dephosphorylates cohesin subunits and prevents Separase from cleaving the Kleisin subunit (Gutierrez-Caballero *et al.*, 2012; Wassmann, 2013; Marston, 2015). We previously observed a reduction in the localization of the PP2A-B56 subunit WDB in a *mei-S332* mutant (Jang *et al.*, 2021). Consistent with this result, WDB recruitment to the kinetochores was abolished by *Spc105R^RNAi* but was present in *Spc105R^C Spc105R^RNAi* oocytes (Figure 4, C and D). These results show that the C-terminal domain of SPC105R is sufficient to recruit PP2A-B56, and thus helps maintain sister-centromere cohesion during meiosis I.

In mouse oocytes, BUB1 has been shown to recruit SGO2 (El Yakoubi *et al.*, 2017). However, *Bub1^RNAi* oocytes did not have a significant defect in MEI-S332 localization (Supplemental Figure S3, A and B), consistent with the observation that *Bub1^RNAi* females were fertile (Wang *et al.*, 2021). In contrast, MEI-S332 localization was re-

duced in *BubR1^RNAi* and *Bub1^RNAi* and *BubR1^RNAi* oocytes and these females were sterile (*Materials and Methods*; Supplemental Figure S3, A and B). Thus, BUBR1 is required to recruit MEI-S332, with possibly a minor contribution from BUB1. Consistent with these findings, we previously showed that BUBR1 is required for PP2A-B56 localization to the kinetochore (Jang *et al.*, 2021). Given the C-terminal domain was sufficient to recruit MEI-S332 and PP2A-B56, we tested whether BUBR1 was recruited to the kinetochore by the C-terminal domain of SPC105R. BUBR1 localization was absent in *Spc105R^RNAi* oocytes. In contrast, BUBR1 localized to the kinetochores in *Spc105R^C Spc105R^RNAi* oocytes (Figure 4, E and F). Thus, the C-terminal domain of SPC105R is sufficient to recruit BubR1, MEI-S332, and PP2A-B56.

Loss of cohesion can be observed by an increase in the number of centromere foci. In wild-type *Drosophila* meiosis I oocytes, eight centromere foci representing the four *Drosophila* chromosomes

FIGURE 3: The SPC105R C-Terminal Domain recruits NDC80. The N-terminal 1284 amino acids of SPC105R is deleted in *Spc105R^C*, retaining only the last 676 amino acids (Figure 1). (A) Confocal images of *Spc105R^RNAi* oocytes expressing the indicated transgene, with DNA (blue), Tubulin (green), centromeres (white), and the kinetochore protein NDC80 (red). Centromeres and NDC80 are shown in separate channels. Scale bars are 5 µm. (B) Quantification of NDC80 intensity at the centromeres in w*ild-type* (n = 68), *Spc105R^RNAi* (n = 77), *Spc105R^B Spc105R^RNAi* (n = 131), and *Spc105R^C Spc105R^RNAi* (n = 107). Error bars indicate SD and **** = *p* value < 0.0001 by an unpaired *t* test. (C) Confocal images of *Spc105R^RNAi* oocytes expressing the indicated transgene, with DNA (blue), Tubulin (green), and centromeres (white). DNA is shown in separate channels. Scale bars are 5 µm. (D) Quantification of end-to-end chromosome length of *wild-type* (n = 34), *Spc105R^RNAi* (n = 12), *Spc105R^C Spc105R^RNAi* (n = 22), and *Spc105R^C Spc105R^RNAi Ndc80^RNAi* (n = 30). Error bars indicate SD, and **** = *p* value < 0.0001 by an unpaired *t* test.

are expected because the sister centromeres are fused. A defect in cohesion results in nine to 16 centromere foci. The number of centromere foci in *Spc105R^C Spc105R^RNAi* oocytes was not significantly different than *Spc105R^B Spc105R^RNAi* oocytes (Figure 4; Supplemental Figure S3C, *p* = 0.14), consistent with the conclusion that the C-terminal domain recruits cohesion protection proteins. *Bub1^RNAi* and *BubR1^RNAi* oocytes had significant defects in sister centromere cohesion (Supplemental Figure S3C). In addition, consistent with redundancy, *Bub1^RNAi* and *BubR1^RNAi* oocytes had a more severe coorientation defect than either single RNAi (Supplemental Figure S3C). These results suggest that BUB1 and BUBR1 have partially overlapping functions in recruiting centromeric cohesion protection proteins.

The role of the N-terminal domain in mediating sister kinetochore coorientation

The second mechanism for maintaining coorientation involves regulating the stability of end-on microtubules attachments to kinetochores. Depletion of PP1-87B, one of three *Drosophila* PP1 alpha-type isoforms, causes a coorientation defect that is independent of Separase and depends on the stabilization of end-on microtubule attachments (Wang *et al.*, 2019; Figure 5, A and B). The SPC105R/KNL1 N-terminal domain has been shown to interact with PP1 (Bajaj *et al.*, 2018). It is not known, however, if the coorientation function of PP1-87B depends on its interaction with SPC105R. Therefore, we tested the hypothesis that the PP1 function in coorientation is mediated by interactions with the N-terminal domain of SPC105R.
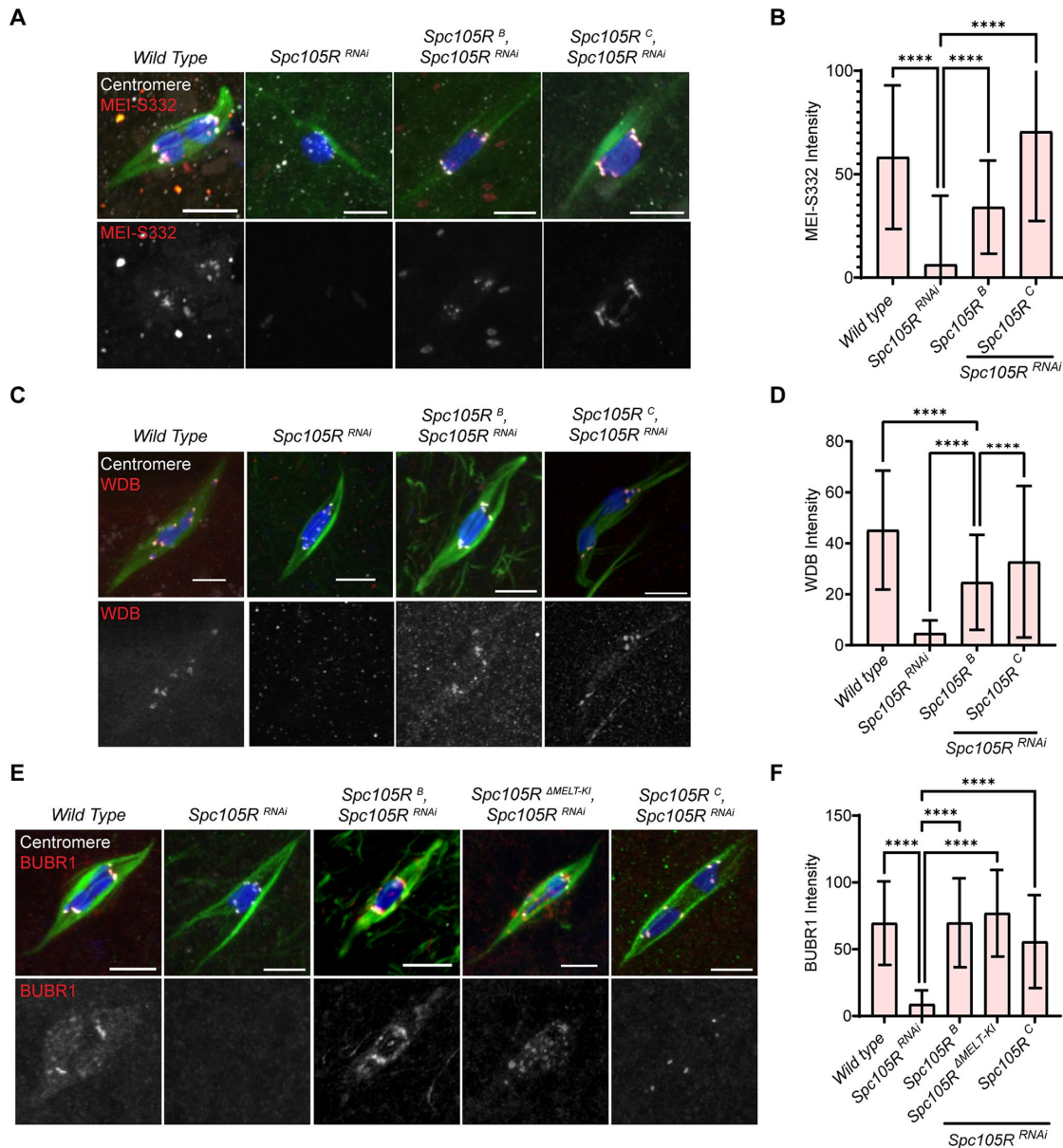
FIGURE 4: The SPC105R C-terminal domain recruits proteins required for centromeric cohesion protection in meiosis I. (A) Confocal images of *Spc105R*^RNAi oocytes expressing the indicated transgene with DNA (blue), Tubulin (green), centromeres (white), and MEI-S332 (red) and shown as a separate channel. Scale bars are 5 μm. (B) Quantification of MEI-S332 intensity at the centromeres for w*ild-type* (*n* = 71), *Spc105R*^RNAi (*n* = 202), *Spc105R^B Spc105R*^RNAi (*n* = 53) and *Spc105R^C Spc105R*^RNAi (*n* = 114). Error bars indicate SD, and **** = *p* value < 0.0001by unpaired *t* test. (C) Confocal images of *Spc105R*^RNAi oocytes expressing the indicated transgene, with DNA (blue), Tubulin (green), centromeres (white), and the PP2A subunit WDB-HA (red), also in a separate channel. Scale bars are 5 μm. (D) Quantification of WDB intensity at the centromeres in w*ild-type* (*n* = 195), *Spc105R^B*, *Spc105R*^RNAi (*n* = 134), *Spc105R*^RNAi (*n* = 189) and *Spc105R^C Spc105R*^RNAi (*n* = 155). Error bars indicate SD and unpaired *t* test **** = *p* value < 0.0001. (E) Confocal images of *Spc105R*^RNAi oocytes expressing the indicated transgene, with DNA (blue), Tubulin (green), centromeres (white), and GFP-BUBR1 (red) and in a separate channel. (F) Quantification of BUBR1 intensity at the centromeres, in *wild-type* (*n* = 247), *Spc105R*^RNAi (*n* = 153), *Spc105R^B Spc105R*^RNAi (*n* = 67), *Spc105R*^MELT-KI *Spc105R*^RNAi (*n* = 89), and *Spc105R^C Spc105R*^RNAi (*n* = 149). Error bars indicate SD and significance is shown by a unpaired *t* test **** = *p* value < 0.0001.

The coorientation defect in *Spc105R*^RNAi oocytes (11.6 centromere foci) was rescued by *Spc105R^B* (Figure 5, A and B; 8.2 centromere foci). A deletion of the entire N-terminal domain, *Spc105R*^ΔN *Spc105R*^RNAi oocytes, had a significant increase in centromere foci, indicating a defect in coorientation. Interestingly, this phenotype was dominant, as a similar increase was observed in the presence of wild-type SPC105R. The coorientation defect in *PP1-87B*^RNAi oocytes is dependent on end-on

microtubule attachments (Wang *et al.*, 2019). We used *Ndc80*^RNAi to eliminate end-on attachments and found that the number of centromere foci was not elevated in *Ndc80*^RNAi, *Spc105R*^ΔN *Spc105R*^RNAi oocytes, and was similar to *Spc105R^B Spc105R*^RNAi oocytes (Figure 5, A and B). The suppression of the centromere foci phenotype is consistent with the conclusion that the coorientation defect in *Spc105R*^ΔN oocytes depends on end-on attachments.
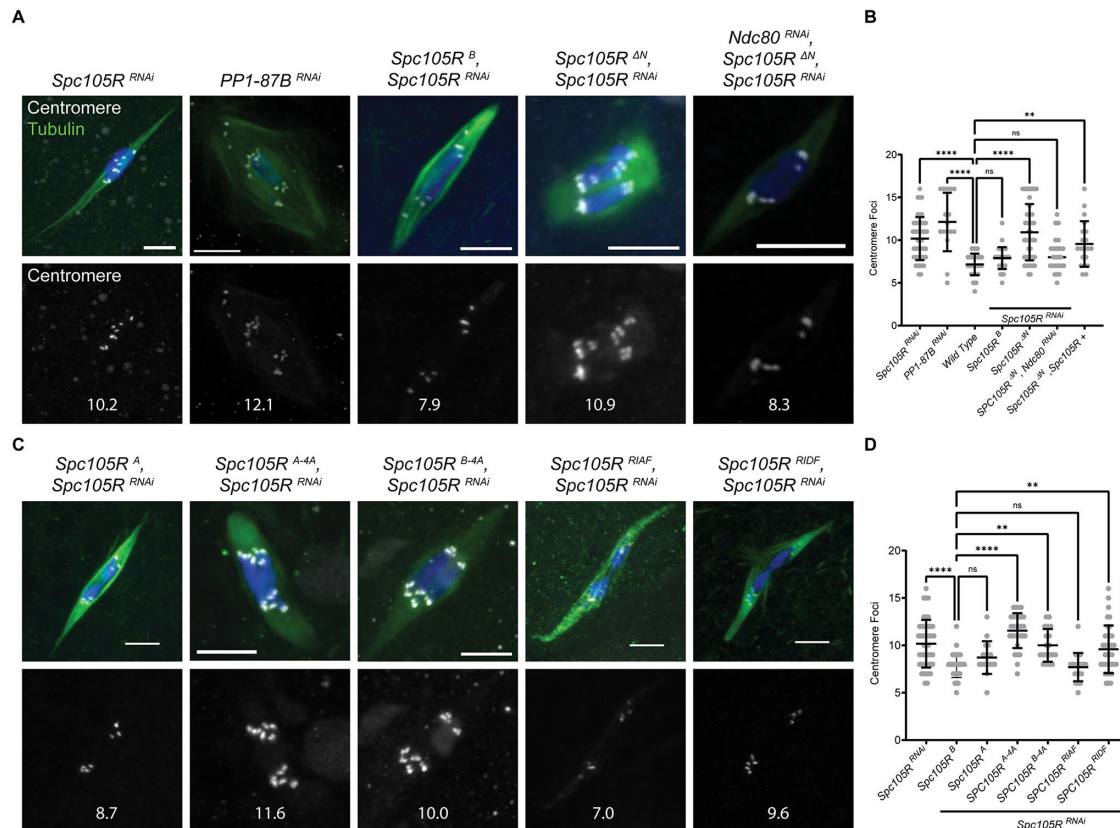
FIGURE 5: The SPC105R N-terminal domain interacts with PP1 to maintain sister centromere coorientation. Mutants with a deletion of the N-terminal domain ($Spc105R^{\Delta N}$) or mutations in the SLRK and RISF sequences are shown in Supplemental Figure S4A. (A) Confocal images of $PP1-87B^{RNAi}$ or $Spc105R^{\Delta N}$ $Spc105R^{RNAi}$ oocytes. Merged images show DNA (blue), Tubulin (green), and centromeres (white). Centromeres are shown in a separate channel along with the average number of foci. Scale bars are 5 µm. (B) Quantification of centromere foci, in the order of the images in A, except *wild-type* not shown. Sample sizes are: 46, 16, 37, 37, 48, 37, and 20, in order of the graph. (C) Confocal images of oocytes where the RISF site was changed to AAAA, RIAF, or RIDF. Centromeres are shown in a separate channel along with the average number of foci. (D) Quantification of centromere foci, in the order of the images in C, except first two shown in A. Sample sizes are: 37, 46, 17, 29, 19, 20, and 36, in order of the graph. Error bars indicate SD and unpaired t test showed significance in number of foci **** $p < 0.0001$, ** $p = 0.001$, ns = not significant.

The N-terminal domain of SPC105R contains two conserved Aurora B/PP1 interaction motifs: SSLRK and RISF. We mutated each site and counted the number of centromere foci to determine whether there was a coorientation defect (Supplemental Figure S4A). In $Spc105R^A$ $Spc105R^{RNAi}$ oocytes, in which the serines in the SSLRK domain are absent, the number of centromere foci was not significantly changed compared with control wild-type oocytes (Figure 5, C and D). In contrast, $Spc105R^{A-4A}$, or $Spc105R^{B-4A}$ $Spc105R^{RNAi}$ oocytes, in which RISF of either the A or B isoforms was changed to AAAA, had a significantly elevated number of centromere foci compared with wild-type oocytes, and were similar to the number of centromere foci in $Spc105R^{\Delta N}$ or $PP1-87B^{RNAi}$ oocytes. These results suggest that the RISF motif regulates centromere coorientation.

To test the effects of phosphorylation and PP1 binding on coorientation, we made phosphomimetic (RIDF) and phosphodefective (RIAF) mutants. We observed that $Spc105R^{RIDF}$ $Spc105R^{RNAi}$, but not $Spc105R^{RIAF}$ $Spc105R^{RNAi}$ oocytes, had significantly increased centromere foci (Figure 5, C and D). These results suggest that loss of PP1 binding, which is the predicted effect of the RIDF, but not the RIAF mutation (Bajaj *et al.*, 2018), may be the main cause of the coorientation defect. The *RIDF* mutant was not viable and sterile while the *RIAF* mutant was viable and fertile (Supplemental

Figure S4D; Table 2), suggesting that the coorientation function is also required in mitosis. In addition, $Spc105R^{RIDF}$ $Spc105R^{RNAi}$ oocytes had unique phenotypes, including tripolar and frayed spindles and evidence of enhanced interactions with the chromosome passenger complex (CPC). The CPC component INCENP is normally located on the central spindle of wild-type oocytes. In $Spc105R^{RIDF}$ $Spc105R^{RNAi}$ oocytes, INCENP also localized at the kinetochores (Supplemental Figure S4B).

$PP1-87B^{RNAi}$ oocytes are also characterized by disorganization of the meiotic chromosomes (Wang *et al.*, 2019). While wild-type oocytes chromosomes cluster together within a single karyosome, $PP1-87B^{RNAi}$ oocytes often have chromosomes separated into multiple groups. This phenotype was also observed in $Spc105R^{\Delta N}$ $Spc105R^{RNAi}$ or $Spc105R^{RIDF}$ $Spc105R^{RNAi}$, and $Spc105R^{RIAF}$ $Spc105R^{RNAi}$ oocytes (Supplemental Figure S4, B and C). These results suggest that maintaining the metaphase I arrest depends on Aurora B, rather than PP1 binding, as with coorientation. We did not observe significant defects in chromosome bi-orientation in the N-terminal domain mutants (Supplemental Figure S5, A and B). Thus, phosphorylation (and PP1 binding) of SSLRK and RISF are implicated in regulating the metaphase I arrest, but not the biorientation of homologous chromosomes during meiosis I.

	Genotype	NDJ %	Total
Spc105R^RNAi and	Spc105R ^B	0.1	2347
	Spc105R ^B-4A	–	sterile
	Spc105R ^A-4A	–	sterile
	Spc105R ^ΔKI	4.6 ****	784
	Spc105R ^ΔMELT	–	sterile
	SPC105R ^RIAF	0.0	322
	Spc105R ^RIDF	–	sterile
No RNAi	Spc105R ^B	0.5	2688
	Spc105R ^B-4A	–	sterile
	Spc105R ^A-4A	0.4	463
	Spc105R ^ΔKI	3.5 ***	544
	Spc105R ^ΔMELT	1.2	276
	Spc105R ^RIAF	0.6	708
	Spc105R ^RIDF	–	sterile

Females expressing the indicated transgene were either in a *Spc105R^RNAi* or wild-type background. Fishers exact test when compared with *Spc105R ^B*, *** = $p = 0.001$, **** = $p < 0.0001$. NDJ = nondisjunction.

TABLE 2: Fertility and nondisjunction in *Spc105R* N-terminal and MELT-KI mutant females.

The role of SPC105R regulatory domains in microtubule attachments

We previously showed that *Spc105R^RNAi* oocytes have a more severe defect in microtubule attachments than *Ndc80^RNAi* oocytes (Radford *et al.*, 2015). In wild-type oocytes, most centromeres associate with the ends of microtubule bundles, which we refer to as end-on attachments (Figure 6A). In *Spc105R^RNAi* oocytes, centromeres are often not associated with any microtubules. In *Ndc80^RNAi* oocytes, the centromeres are usually found adjacent to a bundle of microtubules, with the kinetochores oriented towards the side of the microtubule (Figure 6A; Supplemental Figure S6, A and B). To explain these observations, we proposed that NDC80 is required for end-on microtubule attachments, while SPC105R, which is present in *Ndc80^RNAi* oocytes, is sufficient to mediate lateral microtubule attachments. However, how SPC105R mediates lateral attachments is not known. Therefore, we used two assays to identify the domain(s) of SPC105R that mediate interactions with microtubules.

The first assay for lateral attachments was determining the distance between each kinetochore and the closest the closest bundle of microtubules (measured by tubulin staining). *Spc105R^RNAi* oocytes have a significantly larger average kinetochore-microtubule distance than wild-type or *Ndc80^RNAi* oocytes, indicating they lack the lateral attachments present in *Ndc80^RNAi* oocytes (Supplemental Figure S6). All of the *Spc105R* mutants form end-on attachments through recruitment of NDC80 by the C-terminal domain. Therefore, to analyze lateral microtubule interactions, kinetochore–microtubule distances were measured in a *Ndc80* RNAi background. We predicted that in the absence of both NDC80 and a microtubule binding domain of SPC105R, KT–MT distances would be larger than the distance observed in *Ndc80^RNAi* oocytes, and similar to the distance observed in *Spc105R^RNAi* oocytes. We found that the KT-MT distances in *Ndc80^RNAi* *Spc105R^C* *Spc105R^RNAi* oocytes were similar to the distances in *Spc105R^RNAi* oocytes and significantly larger than the KT–MT distances in *Ndc80^RNAi* oocytes

(Supplemental Figure S6). This indicates that the C-terminal domain of SPC105R does not mediate lateral attachments.

We next tested whether the N-terminal half of SPC105R has a role in lateral attachments by performing this analysis on two deletion mutants. We chose *Spc105R^ΔN* because it deletes a region previously shown to interact with microtubules (Audett *et al.*, 2022). We also chose *Spc105R^ΔMELT-KI* because it showed severe defects in homologues biorientation. We found that the KT–MT distances of both mutants were significantly lower than *Spc105R^RNAi* oocytes, suggesting these two mutants can interact with microtubules. However, the KT–MT distances in *Spc105R^ΔN* *Spc105R^RNAi* and *Spc105R^ΔMELT-KI* *Spc105R^RNAi* were greater than in *Ndc80^RNAi* oocytes, suggesting a defect in microtubule attachments. Because these mutants were not as severe as *Spc105R^C* *Spc105R^RNAi* oocytes, there may be multiple SPC105R domains that mediate lateral attachments.

The second assay was based on an observing whether oocytes entered precious anaphase, which would be indicative of chromosome movement. Oocyte chromosomes enter prometaphase I in a single mass or karyosome. Oocytes lacking chiasma have split karyosomes, suggesting they have precociously entered anaphase (McKim *et al.*, 1993). For example, in *mei-P22* mutants, which lack double-strand-breaks and chiasmata, about 50% of oocytes have split karyosomes (Liu *et al.*, 2002; Figure 6D). Split karyosomes on an elongated spindle were also observed in *mei-P22^–* *Ndc80^RNAi* oocytes, suggesting chromosome movement towards the spindle poles (Figure 6, B and D). In contrast, the frequency of split karyosomes was significantly reduced in *mei-P22^–* *Spc105R^RNAi* oocytes (Figure 6, C and D). These results are consistent with the hypothesis that SPC105R-dependent lateral attachments are sufficient for chromosome movement. We then used this assay to identify the SPC105R domain responsible for lateral attachments. We generated females expressing *Spc105R* mutants in a *mei-P22^–* *Spc105R^RNAi* *Ndc80^RNAi* background. The frequency of split karyosomes was significantly reduced in *Spc105R^C* oocytes (Figure 6, B and D), suggesting a region between amino acids 1 and 1284 mediates chromosome movement. The frequency of split karyosomes was not reduced in *Spc105R^ΔN* oocytes, suggesting that this domain is not required for microtubule interactions. However, this result contrasts with the previous assay, which could be explained whether the N-terminal domain promotes interactions with microtubules that are not capable of movement. Consistent with the first assay, split karyosomes were significantly reduced in *Spc105R^ΔMELT-KI* oocytes, consistent with the previous assay, and suggesting that the region including the MELT- and KI- like repeats between amino acids 123 and 473 are required for chromosome movement, consistent with a role in facilitating lateral attachments to microtubules.

Lateral attachments are not sufficient for biorientation

To test whether SPC105R-mediated lateral attachments are sufficient for biorientation, we compared FISH results in *Ndc80^RNAi* and *Spc105R^RNAi* oocytes. The high frequency of biorientation errors in *Spc105R^RNAi* oocytes was not surprising given the lack of KT–MT attachments (Supplemental Figure S5, C and D). However, *Ndc80^RNAi* oocytes were not significantly better, despite having lateral attachments. Thus, lateral attachments mediated by SPC105R are not sufficient for accurate biorientation of homologous chromosomes at meiosis I.

Dissecting the MELT-KI region

To investigate the functions of the MELT-KI region, we created two mutants with a deletion of each domain. For the KI domain, we
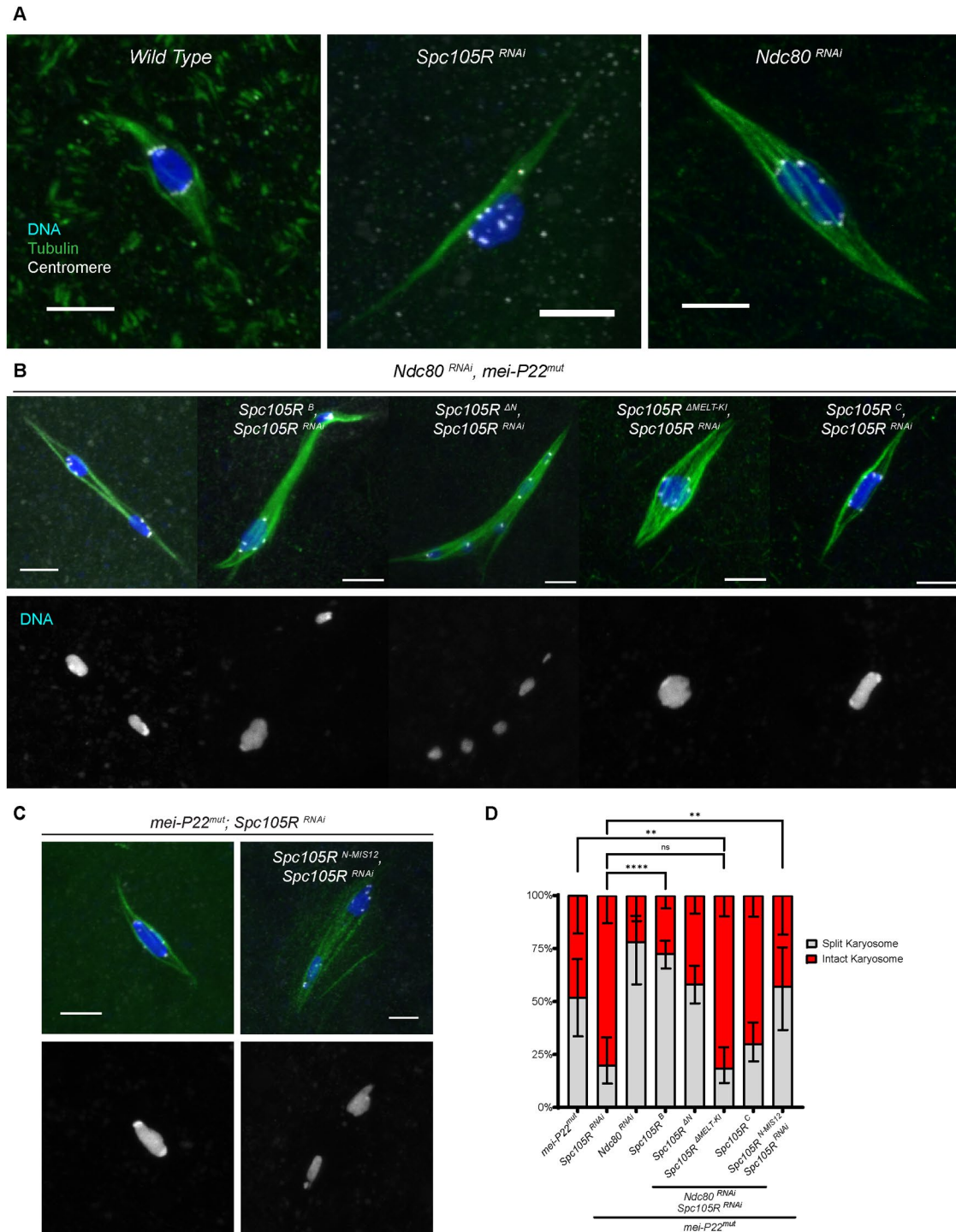
FIGURE 6: SPC105R is sufficient for interactions with spindle microtubules. (A) Confocal images of *wild-type*, *Spc105R^{RNAi}* or *Ndc80^{RNAi}* oocytes. Merged images show DNA (blue), Tubulin (green), and centromeres (white). Scale bars are 5 µm. (B) Oocytes in a *mei-P22* mutant (*mei-P22^{mut}*) background. The first image is only *Ndc80^{RNAi} mei-P22^{mut}*, while the rest express *Ndc80^{RNAi}*, *Spc105R^{RNAi}*, and a *Spc105R* transgene. Due to the absence of crossing over, *mei-P22^{mut}* mutant oocytes fail to arrest in metaphase, and precociously enter anaphase. (C) Oocytes in *mei-P22^{mut}*, *Spc105R* RNAi background. The second image is also expressing a *Spc105R$^{N-mis12}$* transgene. For B and C, merged images show DNA (blue), Tubulin (green), and centromeres (white). Chromosomes are shown in a separate channel. (D) Quantification of the frequency of chromosome separation in oocytes. Sample sizes are: 25, 50, 23, 175, 115, 81, 83, and 21, in order of the graph. Significance in frequency of oocytes entering precocious anaphase determined by Fisher's exact test, with ** = *p* value < 0.01, **** = *p* value < 0.0001, and ns = not significant.
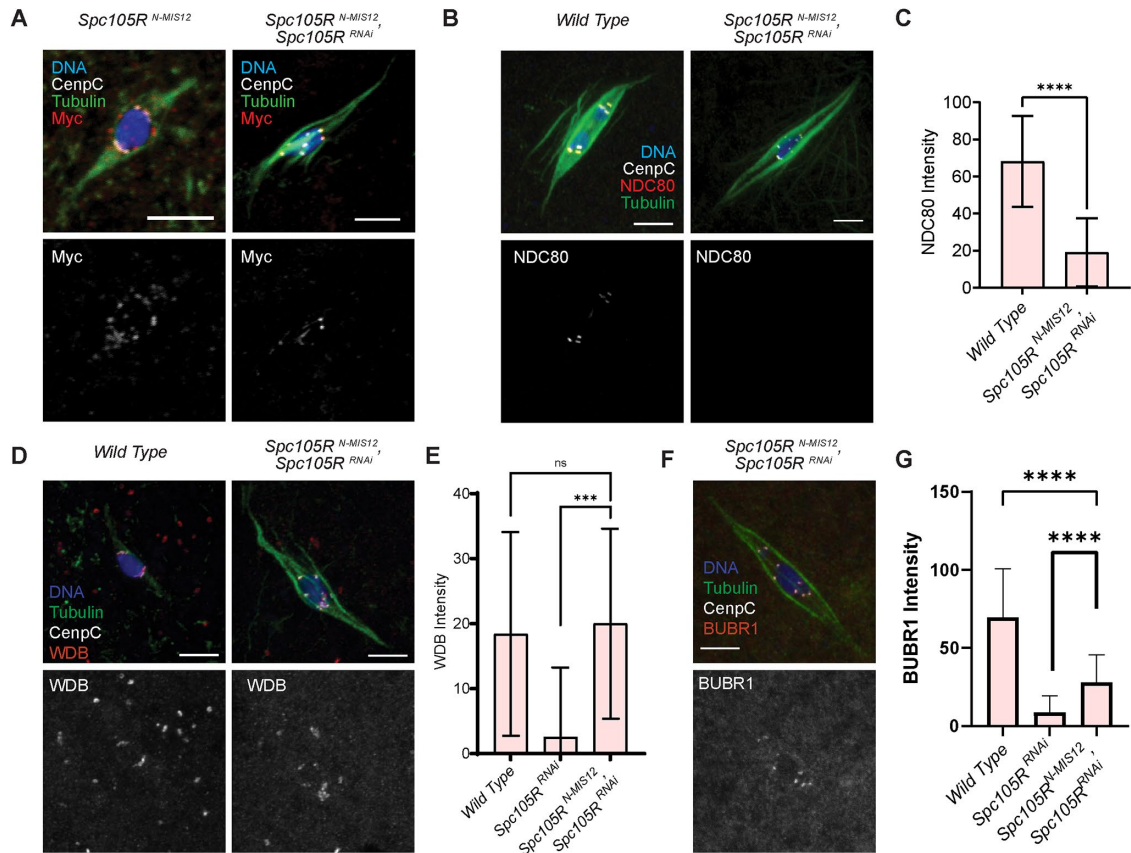
FIGURE 7: The N-terminal domain of SPC105R fused to MIS12 localizes to the kinetochore and recruits PP2A. (A) Confocal images of stage 14 oocytes expressing *Spc105R^N-Mis12*, either in the presence or absence of *Spc105R^RNAi*. The fusion protein contains the first 1284 amino acids of SPC105R followed by all of MIS12, and was detected using an antibody to the myc tag (red). In all images, CENP-C is in white, and tubulin is in green, and the scale bars are 5 μm. (B) Ndc80 (red) does not localize in *Spc105R^N-MIS12 Spc105R^RNAi* oocytes. (C) Measurement of NDC80 intensity in *wild-type* (n = 137) and *Spc105R^N-MIS12 Spc105R^RNAi* (n = 160) oocytes. Error bars indicate SD, and unpaired *t* test showed significance **** = $p < 0.0001$. (D) PP2A-B56 subunit WDB localization shown in red and a separate channel in *wild-type* and *Spc105R^N-MIS12 Spc105R^RNAi* oocytes. (E) Measurement of WDB intensity in wild-type (n = 154), *Spc105R^RNAi* (n = 195), and *Spc105R^N-MIS12 Spc105R^RNAi* (n = 183) oocytes. Error bars indicate SD and unpaired *t* test showed significance, *** = $p < 0.001$ and ns = not significant. (F) GFP-BUBR1 shown in red and in a separate channel in *Spc105R^N-MIS12 Spc105R^RNAi* oocytes. (G) Measurement of BUBR1 intensity in wild-type (n = 117), *Spc105R^RNAi* (n = 153), and *Spc105R^N-MIS12 Spc105R^RNAi* (n = 141) oocytes. Error bars indicate SD and unpaired *t* test showed significance, **** = $p < 0.0001$.

deleted amino acids 247-473 of SPC105R. In these *Spc105R^ΔKI Spc105R^RNAi* oocytes, we did not observe a statistically significant difference in biorientation defects (15% monoorientation) when compared with *Spc105R^B Spc105R^RNAi* (Supplemental Figure S5, A and B). In addition, *Spc105R^ΔKI Spc105R^RNAi* females were viable, fertile, and had a low, but significant, frequency of nondisjunction (Supplemental Figure S4D; Table 2). To examine the function of the MELT-like repeats, we created a *Spc105R^ΔMELT* mutant with a deletion of amino acids 123-246. *Spc105R^ΔMELT Spc105R^RNAi* females were sterile, consistent with a defect in embryonic mitosis. However, these females were viable (Supplemental Figure S4D; Table 2), and the oocytes had an insignificant increase in the frequency of biorientation defects (Supplemental Figure S5B). Thus, relative to the larger deletion of both domains (*Spc105R^ΔMELT-KI*), the *Spc105R^ΔKI* and *Spc105R^ΔMELT* mutants had weaker phenotypes. These results suggest that the MELT and KI domains may function together or additively to facilitate homologous chromosome biorientation in meiosis and possibly also in mitosis.

Testing the function of the N-terminal domain with a fusion to MIS12

To independently test whether the domains of SPC105R not involved in kinetochore assembly are sufficient for microtubule interactions, we fused the N-terminal 1284 amino acids of SPC105R to MIS12. MIS12 is a kinetochore protein recruited by CENP-C that does not depend on SPC105R for localization (Fellmeth *et al.*, 2023). The Myc-fusion protein localized to centromeres in *Spc105R^N-Mis12 Spc105R^RNAi* oocytes (Figure 7A) but failed to recruit NDC80 (Figure 7, B and C). In addition, we observed the staining of SPC105R^N-MIS12 puncta on the spindle, suggesting that aggregates of the mutant kinetochore complex detach from the chromosomes (Figure 7A). This effect was more severe in the presence of wild-type SPC105R, suggesting the interaction between SPC105RN-MIS12 and the centromeres is unstable when there is competition from the wild-type protein or in the presence of end-on attachments.

When expressed with the *mei-P22* mutant, *Spc105RN-Mis12 Spc105R^RNAi* oocytes had split karyosomes, suggesting there were
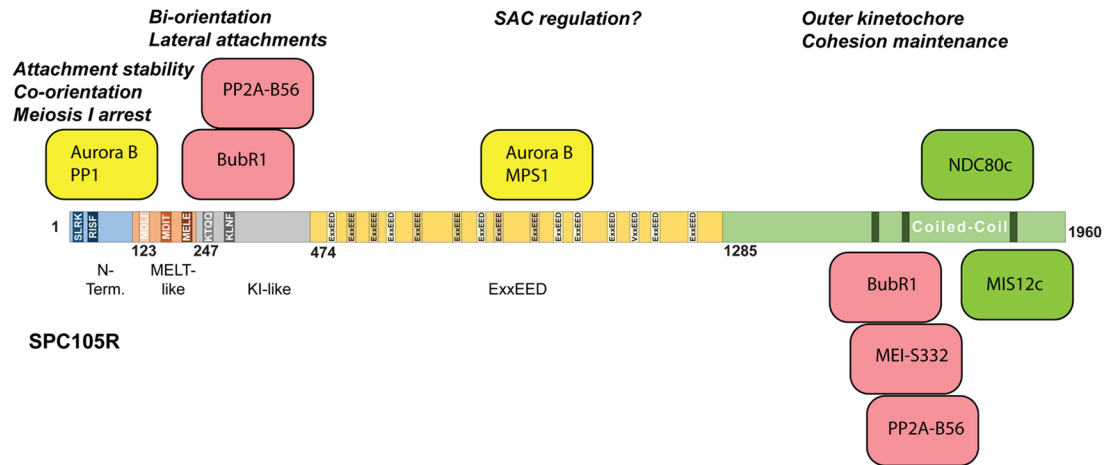
FIGURE 8: Functional domains of SPC105R based on these and prior studies.

lateral attachments between the kinetochores to the microtubules, and chromosome movement towards the poles (Figure 6, B and C). Given the failure to recruit NDC80, the microtubule interactions in these oocytes occur via SPC105R. These results confirm that the N-terminal domain of SPC105R, most likely the MELT-KI region, is sufficient for lateral microtubule interactions and chromosome movement.

We have shown that the C-terminal domain of SPC105R recruits BUBR1 and PP2A-B56. However, the region of vertebrate KNL1 corresponding to MELT-KI in SPC105R has also been shown to recruit BUBR1 and PP2A-B56 (Caldas and DeLuca, 2014; Saurin, 2018). These two results raise the possibility that SPC105R has two BUBR1/PP2A recruitment sites. To test this possibility, we stained *Spc105R^N-Mis12 Spc105R^RNAi* oocytes for WDB, a B56 subunit of PP2A, and BUBR1. These results showed that the *Spc105RN-Mis12 Spc105R^RNAi* oocytes were able to recruit PP2A (Figure 7, D and E), and BUBR1 to the kinetochores (Figure 7, F and G). Combined with experiments using the C-terminal domain (Figure 4), these results indicate that SPC105R has two distinct sites for recruiting BUBR1 and PP2A-B56.

DISCUSSION

A system for studying kinetochore function in *Drosophila* oocytes

SPC105R is at the center of a complex network of signals that regulate microtubule attachments and cell cycle progression (Saurin, 2018). The studies presented here were undertaken to investigate two functions critical for meiotic kinetochores of *Drosophila* oocytes (Figure 8). First, two mechanisms promote coorientation of sister centromeres at meiosis I, cohesion protection and regulating the stability of microtubule attachments (Wang *et al.*, 2019). Second, that SPC105R is sufficient for lateral microtubule attachments (Radford *et al.*, 2015).

Recruitment of the outer kinetochore and cohesion protection

The C-terminal domain of SPC105R is required for kinetochore assembly while the rest of the protein regulates microtubule attachments and the spindle assembly checkpoint. This is consistent with previous studies showing that the NDC80c is recruited by the C-terminal domain of SPC105R/KNL1 in *Drosophila* mitotic cells (Schittenhelm *et al.*, 2009). However, NDC80c can also be recruited by KNL1-independent mechanisms in vertebrate cells, such as the CENP-T pathway (Sridhar and Fukagawa, 2022). These mechanisms

depend on proteins that have not been identified in *Drosophila*. Our results suggest that these other pathways have been lost and SPC105R is the only pathway to assemble NDC80c.

For mitotic cells, protection of cohesins in pericentric regions in critical. The sister kinetochores need to remain separate in order to biorient. Our results provide new insights into the mechanism of maintaining cohesins at meiosis I centromeres, which is important for coorientation by fusing the sister kinetochores (Watanabe, 2012; Nasmyth, 2015). We previously found that SPC105R is required to maintain sister centromere cohesion (Wang *et al.*, 2019; Jang *et al.*, 2021). Here we have shown that the C-terminal domain of SPC105R recruits cohesion protection proteins BubR1, MEI-S332, and PP2A-B56 and is sufficient to maintain sister-centromere cohesion.

Cohesion is established during premeiotic S-phase while SPC105R, like other outer kinetochore proteins, is not recruited to the centromeres until prometaphase. Thus, during a prolonged prophase arrest, the *Drosophila* oocyte must protect centromere cohesion by a kinetochore-independent mechanism. CENP-C may have this role in *Drosophila* (Fellmeth *et al.*, 2023), similar to the role of mammalian and yeast CENP-C in recruiting Moa1 or Meikin (Watanabe, 2012; Nasmyth, 2015). Moa1 and Meikin are not conserved, but *Drosophila* Matrimony may have this role by regulating Polo kinase, which is also required for cohesion maintenance in *Drosophila* (Bonner *et al.*, 2013; Kim *et al.*, 2015; Bonner *et al.*, 2020).

We propose that in meiosis I, SPC105R recruitment of PP2A maintains meiosis I coorientation by providing the cohesion protection that keeps the sister kinetochores fused as a single unit. PP2A may antagonize Polo kinase, which is required for cohesion loss in *Spc105R*-depleted oocytes (Wang *et al.*, 2019) and could be responsible for the phosphorylation event that is required for Separase cleavage of cohesin (Keating *et al.*, 2020). In some mitotic cell types, SGO is recruited to pericentric regions and depends on BUB1 phosphorylation of H2A (Kawashima *et al.*, 2010; Miyazaki *et al.*, 2017). While BUB1 is known to recruit SGO in mouse meiosis (El Yakoubi *et al.*, 2017), *Drosophila* BUB1 knockdown has a surprisingly weak effect on meiosis and viability. BUBR1, on the other hand, had the strongest effect on coorientation, and has been shown to be required for sister chromatid cohesion in *Drosophila* male and female meiosis (Malmanche *et al.*, 2007). BUB1 may have a minor role in cohesion maintenance, based on the observation that the double knockdown of *Bub1* and *BubR1* had the most severe coorientation defect.

Although MEI-332 localizes to metaphase I chromosomes, it is only required for sister chromatid cohesion in meiosis II (Kerrebrock *et al.*, 1995; Tang *et al.*, 1998; Wang *et al.*, 2019). MEI-S332 may be

redundant in meiosis I with Dalmatian (DMT), a Soronin orthologue, in recruiting PP2A-B56 (Yamada *et al.*, 2017; Jang *et al.*, 2021). We do not know whether SPC105R is required to recruit DMT, but the strong cohesion defect in *Spc105R^RNAi* oocytes suggests this may be the case.

The N-terminal domain, checkpoint control, and coorientation

Depletion of PP1-87B in meiosis results in the separation of sister centromeres (a coorientation defect) and chromosomes at metaphase I (Wang *et al.*, 2019). Furthermore, the N-terminal domain of SPC105R has been shown to interact with PP1 in a variety of species (Bajaj *et al.*, 2018; Roy *et al.*, 2019; Audett *et al.*, 2022). We found that deletion of the N-terminal domain or mutations of the RISF motif resulted in a phenotype similar to loss of PP1-87B. The increase in centromere foci observed in oocytes lacking PP1-87B depends on microtubule attachments and is independent of Separase (Wang *et al.*, 2019). These results suggest that the SPC105R-PP1 interaction regulates the stability of microtubule attachments, and this is important for maintaining coorientation.

As done by others in studying the checkpoint response (Rosenberg *et al.*, 2011; Roy *et al.*, 2019), we have characterized phospho-mimetic and -defective mutants to test the effects of Aurora B phosphorylation and PP1 localization on coorientation. Coorientation defects were found in mutants that were predicted to prevent PP1 binding to SPC105R (RIDF and AAAA). In contrast, a mutant preventing Aurora B phosphorylation (RIAF) had mild effects on meiosis, fertility and viability. These results suggest that a defect in PP1 binding, which is blocked by phosphorylation of RISF (Bajaj *et al.*, 2018) or the RIDF mutation, may be the main cause of the coorientation defect. This is consistent with the loss-of-function phenotype of PP1. In addition, the RIDF mutant phenotype showed increased CPC at the centromeres, suggesting PP1 and the CPC compete for binding to the RISF site, or that the CPC is being recruited to correct an attachment defect.

The mechanism of the coorientation and karyosome separation phenotypes is not known. PP1 binding to the RISF motif of SPC105R has been associated with satisfaction of the spindle assembly checkpoint but not error correction (Rosenberg *et al.*, 2011; Espeut *et al.*, 2012; Bajaj *et al.*, 2018; Roy *et al.*, 2019). Our results, specifically that *PP1-87B^RNAi* (Wang *et al.*, 2019) and the RISF mutant oocytes did not have biorientation defects, are consistent with these conclusions. In *Drosophila* mitotic cells, binding of PP1 to the N-terminal domain promotes SAC satisfaction (Audett *et al.*, 2022). Our results suggest that the failure to recruit PP1 results in premature sister centromere and karyosome separation, which is opposite of the expected result if there was a failure to satisfy the SAC. Instead, metaphase I arrest may depend on some of the same signals that trigger anaphase in mitotic cells. This is consistent with the observation that lack of tension on the kinetochores results in premature anaphase (McKim *et al.*, 1993; Jang *et al.*, 1995). Reversal of SAC signaling on metaphase progression may be important for oocytes with natural arrest points. The signals for progression into anaphase in meiosis I may be different than in mitosis and PP1 binding to SPC105R appears to maintain the metaphase I arrest.

Lateral attachments and biorientation

Based on differences between *Spc105^RNAi* and *Ndc80^RNAi* oocytes, we have proposed that SPC105R is sufficient for lateral microtubule attachments (Radford *et al.*, 2015). Lateral attachments with interpolar microtubules can promote biorientation in mitotic (Magidson *et al.*, 2011; Renda *et al.*, 2022) and meiotic cells (Jang *et al.*, 2005;

Kitajima *et al.*, 2011). We have shown here that chromosomes in *Ndc80^RNAi* oocytes can move apart, suggesting there are microtubule attachments that depend on SPC105R. A similar conclusion was made in *Drosophila* mitotic cells (Feijão *et al.*, 2013). Because lateral attachments precede end-on attachments, they could have a significant role in biorientation, for example by preceding and preventing precocious end-on attachments (Muscat *et al.*, 2015; Itoh *et al.*, 2018).

Biorientation was defective in *Ndc80^RNAi* oocytes, indicating that SPC105R-dependent lateral attachments are not sufficient. The requirement of NDC80 in biorientation could include lateral microtubule interactions (Campbell *et al.*, 2019; Doodhi *et al.*, 2021) or recruitment and/or phosphorylation by kinases like MPS1 or AurB (Funabiki, 2019; Sarangapani *et al.*, 2021; Barbosa *et al.*, 2022). Another possibility is that lateral interactions involving interpolar microtubules interact with short NDC80-dependent kinetochores microtubules (Doodhi and Tanaka, 2022). The short kinetochore fibers would give the lateral interactions directionality and perhaps provide a mechanism for biorientation before making end-on attachments (Renda *et al.*, 2022).

The MELT-KI region, or amino acids 124-473, is required for chromosome separation or movement in the *mei-P22* assay, suggesting it has a role in making lateral attachments. Interestingly, the MELT-KI domain is also more important than any other region for biorientation of homologous chromosomes. The *Drosophila* MELT-KI domain contains two components, the first half with the MELT-like motifs, and the second half with KI-like motifs. The presence of 1-3 MELT-like repeats upstream of the KI motifs is a conserved feature of KNL1/SPC105R-like proteins (Tromer *et al.*, 2015), and a vertebrate MELT-KI module was defined as sufficient for SAC activity (Vleugel *et al.*, 2013; Zhang *et al.*, 2014). In our experiments, deletion of either the MELT motifs or the KI-like motifs was less severe than deleting both. Thus, these two components may be part of a single domain required for biorientation of homologous chromosomes, as well as other function in mitosis that contribute to fertility and viability.

With sequences that resemble MELT motifs, the MELT-KI region could interact with MPS1 and Aurora B kinase, proteins known to be required for accurate meiotic chromosome segregation (Gilliland *et al.*, 2007; Colombié *et al.*, 2008; Radford *et al.*, 2012). We have also shown that the N-terminal half of SPC105R, possibly the MELT-KI region, recruits PP2A. This activity could regulate biorientation given that PP2A is required for conversion of lateral to end-on attachments in *Drosophila* oocytes (Jang *et al.*, 2021) and in mitotic cells (Caldas and DeLuca, 2014; Keating *et al.*, 2020). It is also a region that may recruit the motor protein CENP-E, which has also been shown to be required for meiotic chromosome biorientation in *Drosophila* oocytes (Radford *et al.*, 2015) and conversion from lateral to end-on attachments (Shrestha and Draviam, 2013; Huang *et al.*, 2019). Finally, it has been shown that this region recruits the RZZ complex (McGory *et al.*, 2024), which has been proposed to inhibit end-on attachments (Cheerambathur *et al.*, 2013; Barbosa *et al.*, 2022). To understand the mechanism of accurate segregation of chromosomes at meiosis I, it will be important to identify the proteins that interact with this region that are required for biorientation.

MATERIALS AND METHODS
Request a protocol through *Bio-protocol.*

Drosophila genetics and qRT-PCR

Drosophila stocks and crosses were kept at 25°C and maintained on standard media. Many stocks used for experiments were acquired

Genotype	Abbreviation and Reference
P{w+mC= matalpha-GAL-VP16}xV37	matα
P{w[+mC] = tubP-GAL4}LL7	Tub-Gal4
P{TRiP.GL00392}attP2	Spc105R^{RNAi}
P{TRiP.GL00625}attP40	Ndc80^{RNAi}
P{w+mC = UASp-Spc105R}	Spc105R
P{TRiP. HMS00409}	PP1-87B^{RNAi}
P{wrd^{GL00671}wdb^{HMS01864}}	PP2A^{RNAi}
P{BubR1.GFP}	BubR1^{GFP} (Buffin et al., 2005)
M{UAS-wdb.ORF.3xHA.GW}ZH-86Fb	wdb^{HA} (Bischof et al., 2013)
P{TRiP.GLV21065}attP2	BubR1^{RNAi}
P{TRiP.GL00236}attP2	BubR1^{RNAi}
P{TRiP.GL00151}attP2	Bub1^{RNAi} (Wang et al., 2021)

TABLE 3: Drosophila transgenes used in this work.

from the Bloomington Stock Center or from the Harvard Transgenic RNAi Project (TRiP). A list of stocks and their origins is in Table 3. In most experiments, expression of UASP transgenes was induced using P{w[+mC] = matalpha4-GAL-VP16}V37 (referred to as matα). Expression begins during late pachytene in prophase (stage 1), which is after premeiotic DNA replication, and continues through late prophase until the oocyte matures (stage 14; Sugimura and Lilly, 2006; Radford et al., 2012).

To determine the effectiveness of shRNAs in depleting mRNA, total RNA was extracted from oocytes using TRIzol Reagent (Life Technologies) and reverse transcribed into cDNA using the High Capacity cDNA Reverse Transcription Kit (Applied Biosystems). Taq-Man Gene Expression Assays (Life Technologies) were used for qPCR on a StepOnePlus (Life Technologies) real-time PCR system. The shRNA line and percent of wild-type mRNA levels remaining were: Ndc80 GL00625 = 6%, Spc105R GL00392 = 13% (Radford et al., 2015), Bub1 GL00151 = 2% (Wang et al., 2021), BubR1 GLV21065 = 22%, and BubR1 GL00236 = 27%.

Generation of SPC105R transgenes
The Spc105R transgenes were generated from the fully sequenced cDNA clone IP22012, which corresponds to the A splice form (Spc105R^A). The 5'UTR and coding region with the stop codon removed were cloned into the pENTR4 vector. The transgene was made resistant to RNAi by making silent mutations in the sequences complementary to GL00392. The sequence in Spc105R targeted by GL00392, AAGGAGGATAGTTTAGCTAGA, was changed to AAGGAGGACAGCCTGGCCCGC. The difference between the A and B forms is the failure to splice the first intron. The B splice form (Spc105R^B) was generated using site-directed mutagenesis to delete the first intron from the A form (NEB BaseChanger Kit).

All mutants were generated using site directed mutagenesis of the A- or B- form Spc105R coding region in the pENTR4 vector. Wild-type and mutant clones were then subcloned into pPWM using the Clonase reaction (Invitrogen), resulting in fusion of the coding region to six copies of the myc tag in the 3′ end. Constructs of Spc105R with deletions or mutations of these domains were injected into Drosophila melanogaster embryos (Model System Genomics or

BestGene). The linkage of the transgenes was determined and insertions on the third chromosome were recombined onto the same chromosome as the shRNA GL00392.

Analysis of Spc105R mutants
The genetic and cytological phenotypes of each mutant were studied by simultaneous tissue-specific knockdown of endogenous Spc105R by RNAi (Spc105R^{RNAi} oocytes) and expression of a Spc105R transgene. For example, for control experiments we generated females carrying the two UAS transgenes, the shRNA and the wild-type Spc105R, and matα, which will be referred to as Spc105R^B Spc105R^{RNAi} oocytes. Dominant phenotypes were examined by expressing mutant transgene in the absence of the shRNA.

To test for somatic functions such as mitosis, we used P{w[+mC] = tubP-GAL4}LL7 (referred to as Tub:GAL4), which promotes expression in all tissues. Viability of the mutant Drosophila was measured by crossing Spc105R^{RNAi} males to Tub:GAL4/TM3, Sb females. Progeny that inherited the Tub:GAL4 and Spc105R transgenes were expected to survive whether the mutant was functional in mitosis. The Sb progeny (Spc105R, RNAi /TM3, Sb) served as the control because they did not express the transgenes and were expected to survive.

To measure fertility and nondisjunction of the X chromosome, Spc105R^B Spc105R^{RNAi} virgin females were crossed to males with a dominant Bar mutation on the Y chromosome (yw/B^{S}Y). Unique phenotypes for the normal segregation of chromosomes (XX) or (XY), and nondisjunction of the X chromosome, (XO, XXY, XXX, and YO), were scored. XO and XXY progeny are viable whereas XXX and YO are lethal. To calculate nondisjunction rates while taking into account the lethal genotypes, the following equation was used:

$$\frac{\# \ flies \ with \ nondisjunction \times 2}{(\# \ flies \ with \ nondisjunction \times 2) + (\# \ of \ normal \ flies)}.$$

Sterility was defined as no adult progeny from at least 50 females crossed to 50 yw/BSY males, at five females and males per vial.

Immunofluorescence and microscopy
Oocytes in the 14th stage of oocyte development were collected from 2- to 3-day-old, yeast-fed nonvirgin females (Radford and McKim, 2016). These flies were then ground in 1x modified Robb's buffer and filtered through meshes to isolate the stage 14 oocytes. The oocytes were fixed with 5% formaldehyde and heptane before being rinsed in 1X phosphate-buffered saline (PBS). The oocytes were then rolled between glass slides to remove the membranes and incubated for 2 h in PBS/1% Triton X-100 to make them permeable to antibody staining. Afterword, oocytes were washed in PBS/0.05% Triton X-100 and blocked in PTB (0.5% bovine serum albumin and 0.1% Tween-20 in 1X PBS) for 1 h. Subsequently, primary antibodies were added to the oocytes while the secondary antibodies were added to Drosophila embryos to remove any nonspecific binding. After incubating overnight at 4°C, the oocytes were washed in PTB four times at room temperature. The oocytes were incubated with secondary antibodies for 3–4 h at room temperature. The oocytes were then washed in PTB and Hoechst33342 (10 µg/ml) was added to stain the DNA. The oocytes were washed twice more in PTB and then were ready for mounting and imaging.

The primary antibodies used in this paper were mouse antitubulin monoclonal antibody DM1A at 1:50 conjugated to FITC (Sigma-Aldrich), mouse antitubulin monoclonal antibody E7 at 1:200 (Developmental Studies Hybridoma Bank), rat anti-Incenp at 1:600 (Wu et al., 2008), guinea pig anti-CENP-C at 1:1000 (Fellmeth et al., 2023), rat antitubulin YOL1/34 at 1:300 (Millipore), rabbit anti-GFP

at 1:200 (Thermo Fisher Scientific), mouse antimyc 9E10 at 1:50, rabbit anti-SPC105R at 1:4000 (Schittenhelm *et al.*, 2009), mouse anti-SPC105R at 1:200 (this study), rat anti-HA (Clone 3F10, Roche) at 1:50, guinea pig anti-MEI-S332 at 1:5000 (Moore *et al.*, 1998), rabbit anti-NDC80 at 1:500 (Venkei *et al.*, 2011), and rabbit anti-WDB at 1:1000 (Sathyanarayanan *et al.*, 2004). The secondary antibodies used were antiguinea pig 647 at 1:200, antirat Cy3 at 1:200, and antirabbit 488 at 1:200. All the secondary antibodies were from Jackson ImmunoResearch.

To visualize pairs of homologous chromosomes, fluorescent in situ hybridization (FISH) was performed. After fixing the oocytes, 2X SSC was added and the membranes were removed by rolling the oocytes between glass slides. The oocytes were then incubated in increasing concentrations of formamide solution (20, 40, and 50%) before being added to the hybridization solution and probes. The probes recognized the 359 bp repeats on the X chromosome (labeled with AlexaFluor 594), the AACAC repeats on the second chromosome (labeled with Cy3), or the dodeca repeats on the third chromosome (labeled with Alexa 647). This was followed by incubation in 80°C for 20 min and 37°C overnight. The next day, the oocytes were washed in 50% formamide solution twice at 37°C and 20% formamide once at room temperature. The oocytes were then rinsed three times in 2X SSCT (= SSC + 0.1% Tween 20), once in 2X PBST (= PBS + 0.1% Tween20), and incubated in PTB for 4 h at room temperature. Afterward, antitubulin-FITC antibody was added and the oocytes were incubated overnight at room temperature. The next day, the oocytes were washed in PTB and Hoechst33342 (10 µg/ml) was added. After washing twice more in PTB, the oocytes were ready for mounting and imaging. Oocytes were mounted on a glass slide in SlowFade Gold (Invitrogen) and images were taken with a 63x NA 1.4 lens on a Leica SP8 or Stellaris microscope.

Western blots

Stage 14 oocytes collected and membranes removed as for cytology. Fifty milligrams of oocytes were mixed with 350 ul of sodium dodecyl sulfate gel loading buffer, and then ground and boiled. In each lane, 10–15ul of protein was loaded. Transfer to nitrocellulose membranes was done using the BioRad transblot turbo transfer system. The primary antibodies used were rabbit anti-SPC105R (1:5000), mouse anti myc (1:2000), or mouse antitubulin (1:2000). Secondary antibodies were LiCor IRDye 680RD or LT and 800CW used at 1:5000. The secondary antibodies were detected using an Odyssey CLx imager.

Image analysis and statistical analysis

Images were analyzed using Imaris image analysis software (Bitplane) to count centromere foci, measure karyosome length, KT–MT distances, and intensities. To quantify the distance between centromeres and microtubules, spots marking the centromeres and a surface marking the spindle were created. The Distance Transformation Xtension on Imaris was used to measure the distance outside the surface object. GraphPad Prism software was used to perform all statistical tests, and all experiments were repeated at least twice and analyzed for consistency. To measure end-to-end karyosome length, we used the IMARIS software to generate a three-dimensional surface for the karyosome. We placed points in the center of the karyosome surface, parallel to the spindle. We started placing points at one end of the karyosome and finished at the other end and calculated the total distance across all points. For karyosomes with multiple distinct fragments, we measured the total distance across each fragment, parallel to the spindle, and added the distances together for each fragment.

REFERENCES

Audett MR, Johnson EL, McGory JM, Barcelos DM, Szalai EO, Przewloka MR, Maresca TJ (2022). The microtubule- and PP1-binding activities of Drosophila melanogaster Spc105 control the kinetics of SAC satisfaction. Mol Biol Cell 33, ar1.

Bajaj R, Bollen M, Peti W, Page R (2018). KNL1 Binding to PP1 and Microtubules Is Mutually Exclusive. Structure 26, 1327–1336 e1324.

Barbosa J, Sunkel CE, Conde C (2022). The Role of Mitotic Kinases and the RZZ Complex in Kinetochore-Microtubule Attachments: Doing the Right Link. Front Cell Dev Biol 10, 787294.

Bischof J, Bjorklund M, Furger E, Schertel C, Taipale J, Basler K (2013). A versatile platform for creating a comprehensive UAS-ORFeome library in Drosophila. Development 140, 2434–2442.

Bonner AM, Hughes SE, Chisholm JA, Smith SK, Slaughter BD, Unruh JR, Collins KA, Friederichs JM, Florens L, Swanson SK, *et al.* (2013). Binding of Drosophila Polo kinase to its regulator Matrimony is noncanonical and involves two separate functional domains. Proc Natl Acad Sci USA 110, E1222–E1231.

Bonner AM, Hughes SE, Hawley RS (2020). Regulation of Polo Kinase by Matrimony Is Required for Cohesin Maintenance during Drosophila melanogaster Female Meiosis. Curr Biol 30, 715–722. e713.

Buffin E, Lefebvre C, Huang J, Gagou ME, Karess RE (2005). Recruitment of Mad2 to the kinetochore requires the Rod/Zw10 complex. Curr Biol 15, 856–861.

Caldas GV, DeLuca JG (2014). KNL1: bringing order to the kinetochore. Chromosoma 123, 169–181.

Campbell S, Amin MA, Varma D, Bidone TC (2019). Computational model demonstrates that Ndc80-associated proteins strengthen kinetochore-microtubule attachments in metaphase. Cytoskeleton (Hoboken, N.J.) 76, 549–561.

Cheerambathur DK, Gassmann R, Cook B, Oegema K, Desai A (2013). Crosstalk between microtubule attachment complexes ensures accurate chromosome segregation. Science 342, 1239–1242.

Cheeseman IM, Chappie JS, Wilson-Kubalek EM, Desai A (2006). The conserved KMN network constitutes the core microtubule-binding site of the kinetochore. Cell 127, 983–997.

Colombié N, Cullen CF, Brittle AL, Jang JK, Earnshaw WC, Carmena M, McKim K, Ohkura H (2008). Dual roles of Incenp crucial to the assembly of the acentrosomal metaphase spindle in female meiosis. Development 135, 3239–3246.

Costa MFA, Ohkura H (2019). The molecular architecture of the meiotic spindle is remodeled during metaphase arrest in oocytes. J Cell Biol 218, 2854–2864.

Das A, Cesario J, Hinman AM, Jang JK, McKim KS (2018). Kinesin 6 Regulation in Drosophila Female Meiosis by the Non-conserved N- and C- Terminal Domains. G3 (Bethesda, Md.) 8, 1555–1569.

Doodhi H, Kasciukovic T, Clayton L, Tanaka TU (2021). Aurora B switches relative strength of kinetochore-microtubule attachment modes for error correction. J Cell Biol 220, e202011117.

Doodhi H, Tanaka TU (2022). Swap and stop - Kinetochores play error correction with microtubules: Mechanisms of kinetochore-microtubule error correction: Mechanisms of kinetochore-microtubule error correction. Bioessays 44, e2100246.

Dumont J, Desai A (2012). Acentrosomal spindle assembly and chromosome segregation during oocyte meiosis. Trends Cell Biol 22, 241–249.

Dumont J, Oegema K, Desai A (2010). A kinetochore-independent mechanism drives anaphase chromosome separation during acentrosomal meiosis. Nat Cell Biol 12, 894–901.

El Yakoubi W, Buffin E, Cladiere D, Gryaznova Y, Berenguer I, Touati SA, Gomez R, Suja JA, van Deursen JM, Wassmann K (2017). Mps1 kinase-dependent Sgo2 centromere localisation mediates cohesin protection in mouse oocyte meiosis I. Nat Commun 8, 694.

Espeut J, Cheerambathur DK, Krenning L, Oegema K, Desai A (2012). Microtubule binding by KNL-1 contributes to spindle checkpoint silencing at the kinetochore. J Cell Biol 196, 469–482.

Feijão T, Afonso O, Maia AF, Sunkel CE (2013). Stability of kinetochore-microtubule attachment and the role of different KMN network components in Drosophila. Cytoskeleton (Hoboken, N.J.) 70, 661–675.

Fellmeth JE, Jang JK, Persaud M, Sturm H, Changela N, Parikh A, McKim KS (2023). A dynamic population of prophase CENP-C is required for meiotic chromosome segregation. PLoS Genet 19, e1011066.

Funabiki H (2019). Correcting aberrant kinetochore microtubule attachments: a hidden regulation of Aurora B on microtubules. Curr Opin Cell Biol 58, 34–41.

Gilliland WD, Hughes SE, Cotitta JL, Takeo S, Xiang Y, Hawley RS (2007). The multiple roles of mps1 in Drosophila female meiosis. PLoS Genet 3, e113.

Głuszek AA, Cullen CF, Li W, Battaglia RA, Radford SJ, Costa MF, McKim KS, Goshima G, Ohkura H (2015). The microtubule catastrophe promoter Sentin delays stable kinetochore-microtubule attachment in oocytes. J Cell Biol 211, 1113–1120.

Gramates LS, Agapite J, Attrill H, Calvi BR, Crosby MA, dos Santos G, Goodman JL, Goutte-Gattat D, Jenkins VK, Kaufman T, et al. (2022). FlyBase: a guided tour of highlighted features. Genetics 220, iyac035.

Gutierrez-Caballero C, Cebollero LR, Pendas AM (2012). Shugoshins: from protectors of cohesion to versatile adaptors at the centromere. Trends Genet 28, 351–360.

Huang Y, Lin L, Liu X, Ye S, Yao PY, Wang W, Yang F, Gao X, Li J, Zhang Y, et al. (2019). BubR1 phosphorylates CENP-E as a switch enabling the transition from lateral association to end-on capture of spindle microtubules. Cell Res 29, 562–578.

Hughes SE, Miller DE, Miller AL, Hawley RS (2018). Female Meiosis: Synapsis, Recombination, and Segregation in Drosophila melanogaster. Genetics 208, 875–908.

Itoh G, Ikeda M, Iemura K, Amin MA, Kuriyama S, Tanaka M, Mizuno N, Osakada H, Haraguchi T, Tanaka K (2018). Lateral attachment of kinetochores to microtubules is enriched in prometaphase rosette and facilitates chromosome alignment and bi-orientation establishment. Sci Rep 8, 3888.

Jang JK, Gladstein AC, Das A, Shapiro JG, Sisco ZL, McKim KS (2021). Multiple pools of PP2A regulate spindle assembly, kinetochore attachments, and cohesion in Drosophila oocytes. J Cell Sci 134, jcs254037.

Jang JK, Messina L, Erdman MB, Arbel T, Hawley RS (1995). Induction of metaphase arrest in Drosophila oocytes by chiasma-based kinetochore tension. Science 268, 1917–1919.

Jang JK, Rahman T, Kober VS, Cesario J, McKim KS (2007). Misregulation of the Kinesin-like Protein Subito Induces Meiotic Spindle Formation in the Absence of Chromosomes and Centrosomes. Genetics 177, 267–280.

Jang JK, Rahman T, McKim KS (2005). The kinesinlike protein Subito contributes to central spindle assembly and organization of the meiotic spindle in Drosophila oocytes. Mol Biol Cell 16, 4684–4694.

Kawashima SA, Yamagishi Y, Honda T, Ishiguro K, Watanabe Y (2010). Phosphorylation of H2A by Bub1 prevents chromosomal instability through localizing shugoshin. Science 327, 172–177.

Keating L, Touati SA, Wassmann K (2020). A PP2A-B56-Centered View on Metaphase-to-Anaphase Transition in Mouse Oocyte Meiosis I. Cells 9, 390.

Kerrebrock AW, Moore DP, Wu JS, Orr-Weaver TL (1995). Mei-S332, a Drosophila protein required for sister-chromatid cohesion, can localize to meiotic centromere regions. Cell 83, 247–256.

Kim J, Ishiguro K, Nambu A, Akiyoshi B, Yokobayashi S, Kagami A, Ishiguro T, Pendas AM, Takeda N, Sakakibara Y, et al. (2015). Meikin is a conserved regulator of meiosis-I-specific kinetochore function. Nature 517, 466–471.

Kitajima TS (2018). Mechanisms of kinetochore-microtubule attachment errors in mammalian oocytes. Dev Growth Differ 60, 33–43.

Kitajima TS, Ohsugi M, Ellenberg J (2011). Complete kinetochore tracking reveals error-prone homologous chromosome biorientation in mammalian oocytes. Cell 146, 568–581.

Liu H, Jang JK, Kato N, McKim KS (2002). mei-P22 encodes a chromosome-associated protein required for the initiation of meiotic recombination in Drosophila melanogaster. Genetics 162, 245–258.

Liu Y, Petrovic A, Rombaut P, Mosalaganti S, Keller J, Raunser S, Herzog F, Musacchio A (2016). Insights from the reconstitution of the divergent outer kinetochore of Drosophila melanogaster. Open Biol 6, 150236.

Magidson V, O'Connell CB, Loncarek J, Paul R, Mogilner A, Khodjakov A (2011). The spatial arrangement of chromosomes during prometaphase facilitates spindle assembly. Cell 146, 555–567.

Magidson V, Paul R, Yang N, Ault JG, O'Connell CB, Tikhonenko I, McEwen BF, Mogilner A, Khodjakov A (2015). Adaptive changes in the kinetochore architecture facilitate proper spindle assembly. Nat Cell Biol 17, 1134–1144.

Malmanche N, Owen S, Gegick S, Steffensen S, Tomkiel JE, Sunkel CE (2007). Drosophila BubR1 is essential for meiotic sister-chromatid cohesion and maintenance of synaptonemal complex. Curr Biol 17, 1489–1497.

Marston AL (2015). Shugoshins: tension-sensitive pericentromeric adaptors safeguarding chromosome segregation. Mol Cell Biol 35, 634–648.

McAinsh AD, Marston AL (2022). The four causes: The functional architecture of centromeres and kinetochores. Annu Rev Genet 56, 279–314.

McGory JM, Verma V, Barcelos DM, Maresca TJ (2024). Multimerization of a disordered kinetochore protein promotes accurate chromosome segregation by localizing a core dynein module. J Cell Biol 223, e202211122.

McKim KS, Jang JK, Theurkauf WE, Hawley RS (1993). Mechanical basis of meiotic metaphase arrest. Nature 362, 364–366.

Mihajlovic AI, FitzHarris G (2018). Segregating Chromosomes in the Mammalian Oocyte. Curr Biol 28, R895–R907.

Miyazaki S, Kim J, Yamagishi Y, Ishiguro T, Okada Y, Tanno Y, Sakuno T, Watanabe Y (2017). Meikin-associated polo-like kinase specifies Bub1 distribution in meiosis I. Genes Cells 22, 552–567.

Moore DP, Page AW, Tang TT, Kerrebrock AW, Orr-Weaver TL (1998). The cohesion protein MEI-S332 localizes to condensed meiotic and mitotic centromeres until sister chromatids separate. J Cell Biol 140, 1003–1012.

Musacchio A, Desai A (2017). A Molecular View of Kinetochore Assembly and Function. Biology (Basel) 6, 5.

Muscat CC, Torre-Santiago KM, Tran MV, Powers JA, Wignall SM (2015). Kinetochore-independent chromosome segregation driven by lateral microtubule bundles. eLife 4, e06462.

Nasmyth K (2015). A meiotic mystery: How sister kinetochores avoid being pulled in opposite directions during the first division. Bioessays 37, 657–665.

Ogushi S, Rattani A, Godwin J, Metson J, Schermelleh L, Nasmyth K (2021). Loss of sister kinetochore co-orientation and peri-centromeric cohesin protection after meiosis I depends on cleavage of centromeric REC8. Dev Cell 56, 3100–3114. e3104.

Paliulis LV, Nicklas RB (2000). The reduction of chromosome number in meiosis is determined by properties built into the chromosomes. J Cell Biol 150, 1223–1232.

Przewloka MR, Glover DM (2009). The kinetochore and the centromere: A working long distance relationship. Annu Rev Genet 43, 439–465.

Radford SJ, Hoang TL, Głuszek AA, Ohkura H, McKim KS (2015). Lateral and End-On Kinetochore Attachments Are Coordinated to Achieve Bi-orientation in Drosophila Oocytes. PLoS Genet 11, e1005605.

Radford SJ, McKim KS (2016). Techniques for imaging prometaphase and metaphase of meiosis I in fixed Drosophila oocytes. J Vis Exp 116, e54666.

Radford SJ, Jang JK, McKim KS (2012). The Chromosomal Passenger Complex is required for Meiotic Acentrosomal Spindle Assembly and Chromosome Bi-orientation. Genetics 192, 417–429.

Radford SJ, Nguyen AL, Schindler K, McKim KS (2017). The chromosomal basis of meiotic acentrosomal spindle assembly and function in oocytes. Chromosoma 126, 351–364.

Renda F, Miles C, Tikhonenko I, Fisher R, Carlini L, Kapoor TM, Mogilner A, Khodjakov A (2022). Non-centrosomal microtubules at kinetochores promote rapid chromosome biorientation during mitosis in human cells. Curr Biol 32, 1049–1063 e1044.

Rosenberg JS, Cross FR, Funabiki H (2011). KNL1/Spc105 recruits PP1 to silence the spindle assembly checkpoint. Curr Biol 21, 942–947.

Roy B, Verma V, Sim J, Fontan A, Joglekar AP (2019). Delineating the contribution of Spc105-bound PP1 to spindle checkpoint silencing and kinetochore microtubule attachment regulation. J Cell Biol 218, 3926–3942.

Sarangapani KK, Koch LB, Nelson CR, Asbury CL, Biggins S (2021). Kinetochore-bound Mps1 regulates kinetochore-microtubule attachments via Ndc80 phosphorylation. J Cell Biol 220, e202106130.

Sathyanarayanan S, Zheng X, Xiao R, Sehgal A (2004). Posttranslational regulation of Drosophila PERIOD protein by protein phosphatase 2A. Cell 116, 603–615.

Saurin AT (2018). Kinase and Phosphatase Cross-Talk at the Kinetochore. Front Cell Dev Biol 6, 62.

Schittenhelm RB, Chaleckis R, Lehner CF (2009). Intrakinetochore localization and essential functional domains of Drosophila Spc105. EMBO J 28, 2374–2386.

Shrestha RL, Draviam VM (2013). Lateral to end-on conversion of chromosome-microtubule attachment requires kinesins CENP-E and MCAK. Curr Biol 23, 1514–1526.

Sridhar S, Fukagawa T (2022). Kinetochore Architecture Employs Diverse Linker Strategies Across Evolution. Front Cell Dev Biol 10, 862637.

Sugimura I, Lilly MA (2006). Bruno inhibits the expression of mitotic cyclins during the prophase I meiotic arrest of Drosophila oocytes. Dev Cell 10, 127–135.

Tang TT, Bickel SE, Young LM, Orr-Weaver TL (1998). Maintenance of sister-chromatid cohesion at the centromere by the Drosophila MEI-S332 protein. Genes Dev 12, 3843–3856.

Tromer E, Snel B, Kops GJ (2015). Widespread Recurrent Patterns of Rapid Repeat Evolution in the Kinetochore Scaffold KNL1. Genome Biol Evol 7, 2383–2393.

Venkei Z, Przewloka MR, Glover DM (2011). Drosophila Mis12 complex acts as a single functional unit essential for anaphase chromosome movement and a robust spindle assembly checkpoint. Genetics 187, 131–140.

Vleugel M, Tromer E, Omerzu M, Groenewold V, Nijenhuis W, Snel B, Kops GJ (2013). Arrayed BUB recruitment modules in the kinetochore scaffold KNL1 promote accurate chromosome segregation. J Cell Biol 203, 943–955.

Wang LI, Das A, McKim KS (2019). Sister centromere fusion during meiosis I depends on maintaining cohesins and destabilizing microtubule attachments. PLoS Genet 15, e1008072.

Wang LI, DeFosse T, Jang JK, Battaglia RA, Wagner VF, McKim KS (2021). Borealin directs recruitment of the CPC to oocyte chromosomes and movement to the microtubules. J Cell Biol 220, e202006018.

Wassmann K (2013). Sister chromatid segregation in meiosis II: deprotection through phosphorylation. Cell Cycle 12, 1352–1359.

Watanabe Y (2012). Geometry and force behind kinetochore orientation: lessons from meiosis. Nat Rev Mol Cell Biol 13, 370–382.

Webster A, Schuh M (2017). Mechanisms of Aneuploidy in Human Eggs. Trends Cell Biol 27, 55–68.

Wignall SM, Villeneuve AM (2009). Lateral microtubule bundles promote chromosome alignment during acentrosomal oocyte meiosis. Nat Cell Biol 11, 839–844.

Wu C, Singaram V, McKim KS (2008). mei-38 is required for chromosome segregation during meiosis in Drosophila females. Genetics 180, 61–72.

Yamada T, Tahara E, Kanke M, Kuwata K, Nishiyama T (2017). Drosophila Dalmatian combines sororin and shugoshin roles in establishment and protection of cohesion. EMBO J 36, 1513–1527.

Yoshida S, Kaido M, Kitajima TS (2015). Inherent Instability of Correct Kinetochore-Microtubule Attachments during Meiosis I in Oocytes. Dev Cell 33, 589–602.

Zhang G, Lischetti T, Nilsson J (2014). A minimal number of MELT repeats supports all the functions of KNL1 in chromosome segregation. J Cell Sci 127, 871–884.